Role of meson interactions in the $D_s^+ \to \pi^+\pi^+\pi^-\eta$ decay

Jing Song,[1,2,3,*] A. Feijoo,[3,†] and E. Oset[3,‡]

[1]*School of space and environment, Beihang University, Beijing 102206, People's Republic of China*
[2]*School of Physics, Beihang University, Beijing 102206, People's Republic of China*
[3]*Departamento de Física Teórica and IFIC, Centro Mixto Universidad de Valencia-CSIC, Institutos de Investigación de Paterna, Apartado 22085, 46071 Valencia, Spain*

(Received 20 May 2022; accepted 4 October 2022; published 28 October 2022)

We perform a theoretical study of the $D_s^+ \to \pi^+\pi^+\pi^-\eta$ decay. We look first at the basic D_s^+ decay at the quark level from external and internal emission. Then we hadronize a pair or two pairs of $q\bar{q}$ states to have mesons at the end. Posteriorly the pairs of mesons are allowed to undergo final state interaction, by means of which the $a_0(980)$, $f_0(980)$, $a_1(1260)$, and $b_1(1235)$ resonances are dynamically generated. The G parity is used as a filter of the possible channels, and from those with negative G parity only the ones that can lead to $\pi^+\pi^+\pi^-\eta$ at the final state are kept. Using transition amplitudes from the chiral unitary approach that generates these resonances and a few free parameters, we obtain a fair reproduction of the six mass distributions reported in the BESIII experiment.

DOI: 10.1103/PhysRevD.106.074027

I. INTRODUCTION

D meson decays into three mesons have long being considered of good source of information to study the interaction of mesons [1–14] (see the review in [15]). The scattering mechanisms of final meson pairs are usually investigated in these works trying to obtain information on this interaction and resonances formed in the process. The D decay into four mesons introduces a challenging task due to the additional meson pairs that require a consideration. In this paper we wish to do such a theoretical work on the $D_s^+ \to \pi^+\pi^+\pi^-\eta$ reaction measured for the first time in [16] by the BESIII Collaboration. One intriguing aspect of the analysis of [16] is the claim that the $D_s^+ \to a_0^+(980)\rho^0$ decay mode proceeds via weak annihilation, with a rate about 1 order of magnitude bigger than ordinary weak-annihilation processes. In the order of the relevance of different weak decay mechanisms, weak annihilation goes below external emission, internal emission, and W exchange [17,18]. Hence, observing a reaction which proceeds via this mode with exceptionally large strength is certainly a relevant finding. Yet, there might be some ways to produce this mode indirectly, producing other intermediate states that lead to the desired final state through strong interaction transitions in the final states. This is one of the issues that we investigate here.

It is not the first time that such a thing happens, since in the study of $D_s^+ \to \pi^+\pi^0\eta$ decay [19], the $\pi^+ a_0(980)$ decay mode was also branded as an example of weak annihilation with an abnormally large strength. Yet, in Ref. [10] it was found that the process could be explained through a mechanism of internal emission, through the production of $K\bar{K}$ and the subsequent $K\bar{K} \to \pi\eta$ transition, dominated by the $a_0(980)$ resonance. An alternative explanation was provided in [11] through a triangle mechanism where one has $D_s \to \rho^+\eta$, which proceeds via external emission, followed by $\rho \to \pi\pi$ and a fusion of $\pi\eta$ to give the $a_0(980)$ resonance. The same argumentation was followed in [20], where the work of [19] was discussed and other possible mechanisms were considered. What is clear is that with either of the mechanisms of [10,11,20] one does not need weak annihilation for the $D_s \to \pi a_0(980)$ production, and the strong interaction of the resulting mesons can lead to the desired final state. We will find a similar situation in the present reaction, where considering mechanisms of external and internal emission of different intermediate particles and allowing them to make transitions through final state interaction, we can obtain the desired final state.

So far there is only one theoretical work which pays attention to this reaction [21]. The work looks only to two particular decay channels, $D_s \to \rho^0 a_0^+(980) \to \rho\pi\eta$ and $D_s \to \rho^+ a_0^0(980) \to \rho^+ K^+ K^-$, using a triangle diagram like $D_s \to \pi\eta$ (virtual $\pi \to \pi\rho$), and a fusion of $\pi\eta$ to give the $a_0(980)$ resonance. A similar mechanism with $K^+\bar{K}^0$

*song-jing@buaa.edu.cn
†edfeijoo@ific.uv.es
‡oset@ific.uv.es

intermediate states in the loop instead of two pions is also considered. In both cases the primary products of the decay have a much smaller mass than the final ones, forcing them to be highly off shell. The work of [21] finds reasonable results for the cases of $D_s \to \rho^0 a^+ \to \rho\pi\eta$ decay compared with the analysis of [16], but with a rate for $D_s \to \rho^+ a_0^0$ ($a_0 \to K^+K^-$) 1 order of magnitude smaller. They hint at a possible misinterpretation of the data of [16] due to a possible contribution of $D_s \to f_0(980)\rho^+$.

Our aim in the present work is more ambitious, since we want to reproduce the six invariant mass distributions that have been reported in [16], $M_{\pi^+\pi^+}$, $M_{\pi^+\pi^-}$, $M_{\pi^+\eta}$, $M_{\pi^-\eta}$, $M_{\pi^+\pi^+\pi^-}$, and $M_{\pi^+\pi^-\eta}$. The methodology is also different, we look at the reaction from the perspective that the different resonances that are observed in the analysis of the reaction, $f_0(500)$, $f_0(980)$, $a_0(980)$, and $a_1(1260)$, are obtained within the chiral unitary approach from the interaction of different mesons. In this sense, the scalar resonances $f_0(500)$, $f_0(980)$, and $a_0(980)$ are obtained from the interaction of pairs of pseudoscalar mesons in coupled channels [22–25], while the $a_1(1260)$ and other axial vector mesons are obtained from the interaction of the pairs of a pseudoscalar and a vector meson [26–29]. Then our procedure is as follows: we consider all possible decay mechanisms at the quark level and then proceed to create vectors and a pseudoscalar recurring to the hadronization of $q\bar{q}$ pairs into a pair of mesons, pseudoscalar-pseudoscalar (PP), or vector-pseudoscalar (VP). After this, we allow the different PP or VP pairs to interact, leading to the $\pi^+\pi^+\pi^-\eta$ configuration finally. In the process of interaction, different resonances are produced which are clearly visible in the different mass distributions. Our approach contains a few free parameters related to the strength of the different primary production processes, for which the order of magnitude is known, and a good reproduction of the six invariant mass distributions is obtained with considerably less freedom than in the partial wave analysis done in the experiment [16]. The relevant role played by the different resonances is then exposed.

TABLE I. G parity acting on K and K^* states.

	K^+	K^0	$\bar{K}^0$	K^-	K^{*+}	K^{*0}	$\bar{K}^{*0}$	K^{*-}
$G(K_i)$	$\bar{K}^0$	$-K^-$	$-K^+$	K^0	$-\bar{K}^{*0}$	K^{*-}	K^{*+}	$-K^{*0}$

II. FORMALISM

A. G parity of the process

The first realization in the $D_s^+ \to \pi^+\pi^+\pi^-\eta$ reaction is that the G parity of the final state is negative. Hence, after the weak interaction and prior to any final state interaction, we must select only states where G parity is negative. Pseudoscalar mesons and vector mesons without strangeness have given G parity, η, ρ positive, π, ω, ϕ negative. K or K^* have no G parity but pairs of them can have it. The G parity is defined as

$$G = Ce^{-i\pi I_2}; \qquad e^{-i\pi I_2}|I, I_3\rangle = (-1)^{I-I_3}|I, -I_3\rangle. \quad (1)$$

With our isospin doublet convention (K^+, K^0), $(\bar{K}^0, -K^-)$ and $CK^+ = K^-$, $CK^0 = \bar{K}^0$, (K^{*+}, K^{*0}), $(\bar{K}^{*0}, -K^{*-})$ and $CK^{*+} = -K^{*-}$, $CK^{*0} = -\bar{K}^{*0}$, we have the G parity acting over the K, K^* states as shown in Table I.

B. External emission with one hadronization

We show in Fig. 1 the Cabibbo favored process of external emission at the quark level. Since we need four particles in the final states we need to produce a vector meson, which will decay to two pseudoscalars, and a pair of pseudoscalars. We have several options:

(1) Hadronize $\bar{d}u$ with PP and $s\bar{s}$ giving a vector;
(2) Produce a vector from $\bar{d}u$ and hadronize $s\bar{s}$ to two pseudoscalars;
(3) Hadronize $\bar{d}u$ with VP or PV and $s\bar{s}$ to two pseudoscalars;
(4) Hadronize $\bar{s}s$ to VP or PV and $\bar{d}u$ a pseudoscalar.

Let us see the consequences. For this we would need the representation of $q\bar{q}$ in terms of mesons, which is given by

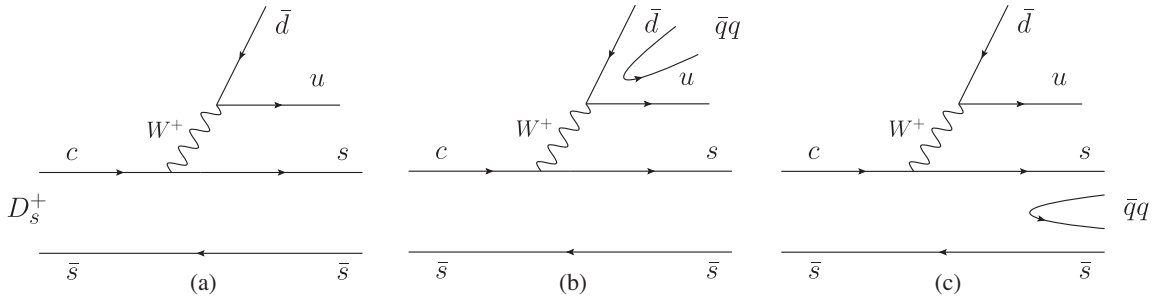

FIG. 1. External emission mechanism for the D_s^+ decay at the quark level. (a) Basic mechanism, (b) hadronization of the $u\bar{d}$ component, (c) hadronization of the $s\bar{s}$ component.

$$P=\begin{pmatrix} \frac{\pi^0}{\sqrt{2}}+\frac{\eta}{\sqrt{3}}+\frac{\eta'}{\sqrt{6}} & \pi^+ & K^+ \\ \pi^- & \frac{-\pi^0}{\sqrt{2}}+\frac{\eta}{\sqrt{3}}+\frac{\eta'}{\sqrt{6}} & K^0 \\ K^- & \bar{K}^0 & -\frac{\eta}{\sqrt{3}}+\frac{2\eta'}{\sqrt{3}} \end{pmatrix}, \quad (2)$$

$$V=\begin{pmatrix} \frac{\rho^0}{\sqrt{2}}+\frac{\omega}{\sqrt{2}} & \rho^+ & K^{*+} \\ \rho^- & \frac{-\rho^0}{\sqrt{2}}+\frac{\omega}{\sqrt{2}} & K^{*0} \\ K^{*-} & \bar{K}^{*0} & \phi \end{pmatrix}, \quad (3)$$

where we have taken the ordinary $\eta-\eta'$ mixing of Ref. [30].

Let us see what one obtains with the four options above. (We neglect η' which plays no role in these processes.)

(1)

$$u\bar{d}\to\sum_i u\bar{q}_i q_i\bar{d}=\sum_i P_{1i}P_{i2}=(P^2)_{12}$$
$$=\left(\frac{\pi^0}{\sqrt{2}}+\frac{\eta}{\sqrt{3}}\right)\pi^+ +\pi^+\left(\frac{-\pi^0}{\sqrt{2}}+\frac{\eta}{\sqrt{3}}\right)+K^+\bar{K}^0. \quad (4)$$

On the other hand, the vector for $s\bar{s}$ is ϕ which decays to $K\bar{K}$ but not to $\pi^+\pi^-$ (different G parity). Hence, this process cannot lead to our final state of $\pi^+\pi^+\pi^-\eta$.

(2)

$$s\bar{s}\to\sum_i s\bar{q}_i q_i\bar{s}=\sum_i P_{3i}P_{i3}=(P^2)_{33}$$
$$=K^-K^+ +\bar{K}^0K^0+\frac{\eta\eta}{3} \quad (5)$$

and $\bar{d}u$ as a vector is ρ^+. The vector ρ^+ can give $\pi^+\pi^0$ but $s\bar{s}$ has $I=0$ and hadronization does not change the isospin, which means that the combination of Eq. (5) cannot give $\pi^0\eta$. Once again, this mechanism cannot produce our final state.

(3a) We hadronize $u\bar{d}$ with VP and have

$$u\bar{d}\to\sum_i u\bar{q}_i q_i\bar{d}=\sum_i V_{1i}P_{i2}=(VP)_{12}$$
$$=\left(\frac{\rho^0}{\sqrt{2}}+\frac{\omega}{\sqrt{2}}\right)\pi^+ +\rho^+\left(\frac{-\pi^0}{\sqrt{2}}+\frac{\eta}{\sqrt{3}}\right)+K^{*+}\bar{K}^0 \quad (6)$$

and $s\bar{s}$ will give rise to the η. According to the $\eta-\eta'$ mixing of Ref. [30] one has

$$s\bar{s}=-\frac{1}{\sqrt{3}}\eta+\sqrt{\frac{2}{3}}\eta'. \quad (7)$$

We can see that there are already candidates, since $\rho^0\to\pi^+\pi^-$ and we can have $\pi^+\pi^+\pi^-\eta$.

(3b) We hadronize $u\bar{d}$ with PV and have

$$u\bar{d}\to\sum_i u\bar{q}_i q_i\bar{d}=\sum_i P_{1i}V_{i2}=(PV)_{12}$$
$$=\left(\frac{\pi^0}{\sqrt{2}}+\frac{\eta}{\sqrt{3}}\right)\rho^+ +\pi^+\left(\frac{-\rho^0}{\sqrt{2}}+\frac{\omega}{\sqrt{2}}\right)+K^+\bar{K}^{*0} \quad (8)$$

and once again with $\rho^0\to\pi^+\pi^-$, the extra π^+, and η from $s\bar{s}$, the combination can give the desired final state.

Now, an inspection of Eqs. (6) and (8) shows immediately that these states mix the G parity, which is not surprising since they come from a weak process that does not conserve isospin. However, we can make good G-parity states by means of the linear combinations $(VP\pm PV)$. Indeed,

$$(VP)_{12}-(PV)_{12}=\sqrt{2}\rho^0\pi^+-\sqrt{2}\rho^+\pi^0+K^{*+}\bar{K}^0-K^+\bar{K}^{*0} \quad (9)$$

$$(VP)_{12}+(PV)_{12}=\sqrt{2}\omega\pi^+ +\frac{2}{\sqrt{3}}\rho^+\eta+K^{*+}\bar{K}^0+K^+\bar{K}^{*0}. \quad (10)$$

If we look at Table I we can see that $(VP)_{12}-(PV)_{12}$ has negative G parity, while $VP+PV$ has positive G parity. Hence, it is the $(VP-PV)_{12}$ combination of Eq. (9), the one we shall take to produce the final state $\pi^+\pi^+\pi^-\eta$. Thus, we consider the state

$$|HE3'\rangle=(VP-PV)_{12}$$
$$=-\frac{1}{\sqrt{3}}\eta(\sqrt{2}\rho^0\pi^+-\sqrt{2}\rho^+\pi^0+K^{*+}\bar{K}^0-K^+\bar{K}^{*0}) \quad (11)$$

but the $\rho^+\pi^0\eta$ combination going to $\pi^+\pi^0\pi^0\eta$ will not contribute. We can therefore take

$$|HE3\rangle=-\sqrt{\frac{2}{3}}\eta\rho^0\pi^+-\frac{1}{\sqrt{3}}\eta(K^{*+}\bar{K}^0-K^+\bar{K}^{*0}) \quad (12)$$

(4a)

$$s\bar{s}\to\sum_i s\bar{q}_i q_i\bar{s}=\sum_i V_{3i}P_{i3}=(VP)_{33}$$
$$=K^{*-}K^+ +\bar{K}^{*0}K^0-\phi\frac{\eta}{\sqrt{3}} \quad (13)$$

and $\bar{d}u$ will be a π^+. By looking again to Table I we can see that the former combination together with π^+ has not a well-defined G parity.

TABLE II. Nonstrange axial vector resonances generated by the VP, PV interaction [26,27].

	$h_1(1173)$	$h_1(1380)$	$b_1(1235)$	$a_1(1260)$	$f_1(1285)$
I^G	0^-	0^-	1^+	1^-	0^+

(4b)

$$s\bar{s} \to \sum_i s\bar{q}_i q_i \bar{s} = \sum_i P_{3i} V_{i3} = (PV)_{33} = K^- K^{*+} + \bar{K}^0 K^{*0} - \phi\frac{\eta}{\sqrt{3}} \tag{14}$$

which, again, has no defined G parity.

We construct the $VP \pm PV$ combinations and find

$$(VP)_{33} - (PV)_{33} = K^{*-}K^+ - K^- K^{*+} + \bar{K}^{*0}K^0 - \bar{K}^0 K^{*0} \tag{15}$$

$$(VP)_{33} + (PV)_{33} = K^{*-}K^+ + K^- K^{*+} + \bar{K}^{*0}K^0 + \bar{K}^0 K^{*0} - \frac{2}{\sqrt{3}}\phi\eta \tag{16}$$

Once again we see that the $VP - PV$ combination together with π^+ has G parity negative, while $VP + PV$ and π^+ has G parity positive. We can think of making the transition of $(VP - PV)_{33}$ to $\rho^0\eta$ to complete $\rho^0\eta\pi^+ \to \pi^+\pi^-\eta\pi^+$. However, this is not possible since the combination $VP - PV$, coming from $s\bar{s}$, has $I = 0$ and hence cannot go to $\rho\eta$. Indeed, the $I^G = 0^+$ resonance coming from $VP - PV$ combinations is the $f_1(1285)$ (see Table II), which only couples to $K^*\bar{K}$, $\bar{K}^* K$ channels [27,29]. Thus, from all possible states coming from hadronization with external emission, only one, $|HE3\rangle$ of Eq. (12), can lead to our desired final state.

C. Internal emission with one hadronization

We look now at the process of Fig. 2 for the D_s^+ decay, We follow now the same strategy as before:

(1) Hadronize $s\bar{d}$ with PP and $u\bar{s}$ is a vector;
(2) Hadronize $u\bar{s}$ to PP and $s\bar{d}$ is a vector;
(3) Hadronize $s\bar{d}$ to VP, PV and $u\bar{s}$ is a pseudoscalar;
(4) Hadronize $u\bar{s}$ to VP, PV and $s\bar{d}$ is a pseudoscalar.

Let us see these possibilities in detail.

(1)

$$s\bar{d} \to \sum_i s\bar{q}_i q_i \bar{d} = \sum_i P_{3i}P_{i2} = (P^2)_{32} = K^-\pi^+ + \left(-\frac{\pi^0}{\sqrt{2}} + \frac{\eta}{\sqrt{3}}\right)\bar{K}^0 - \frac{\eta}{\sqrt{3}}\bar{K}^0 = K^-\pi^+ - \frac{\pi^0}{\sqrt{2}}\bar{K}^0 \tag{17}$$

and the $u\bar{s}$ component gives K^{*+}.

(2)

$$u\bar{s} \to \sum_i u\bar{q}_i q_i \bar{s} = \sum_i P_{1i}P_{i3} = (P^2)_{13} = \left(\frac{\pi^0}{\sqrt{2}} + \frac{\eta}{\sqrt{3}}\right)K^+ + \pi^+ K^0 - \frac{\eta}{\sqrt{3}}K^+ = \frac{\pi^0}{\sqrt{2}}K^+ + \pi^+ K^0 \tag{18}$$

and the $s\bar{d}$ component gives $\bar{K}^{*0}$. Neither $(P^2)_{32}K^{*+}$ nor $(P^2)_{13}\bar{K}^{*0}$ have good G parity, but we make again the combinations

$$(P^2)_{32}K^{*+} - (P^2)_{13}\bar{K}^{*0} = \left(K^-\pi^+ - \bar{K}^0\frac{\pi^0}{\sqrt{2}}\right)K^{*+} - \left(\frac{\pi^0}{\sqrt{2}}K^+ + \pi^+K^0\right)\bar{K}^{*0} = \pi^+(K^{*+}K^- - \bar{K}^{*0}K^0) - \frac{\pi^0}{\sqrt{2}}(K^{*+}\bar{K}^0 + \bar{K}^{*0}K^+) \tag{19}$$

$$(P^2)_{32}K^{*+} + (P^2)_{13}\bar{K}^{*0} = \left(K^-\pi^+ - \bar{K}^0\frac{\pi^0}{\sqrt{2}}\right)K^{*+} + \left(\frac{\pi^0}{\sqrt{2}}K^+ + \pi^+K^0\right)\bar{K}^{*0} = \pi^+(K^{*+}K^- + \bar{K}^{*0}K^0) + \frac{\pi^0}{\sqrt{2}}(\bar{K}^{*0}K^+ - K^{*+}\bar{K}^0). \tag{20}$$

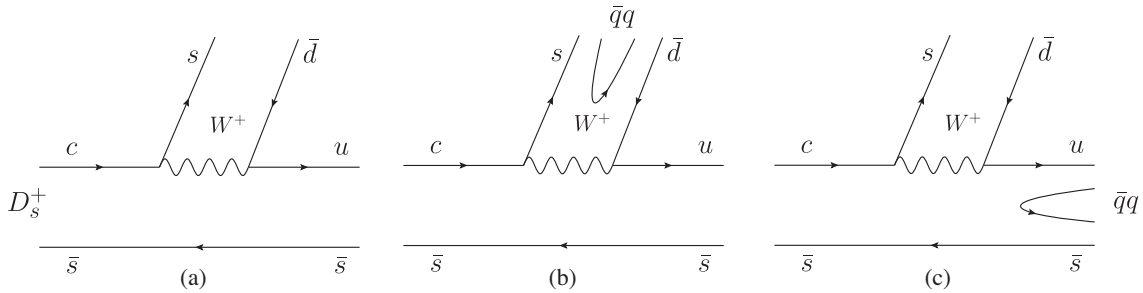

FIG. 2. Internal emission mechanism for D_s^+ decay at the quark level. (a) Basic mechanism, (b) hadronization of the $s\bar{d}$ component, (c) hadronization of the $u\bar{s}$ component.

By looking at Table I, we see that the (−) combination has G parity negative, while the (+) combination has G parity positive. Note also that since we have produced the quarks $s\bar{s}\,\bar{d}\,u$ in Fig. 2, this has $|I, I_3\rangle = |1, 1\rangle$ for all the combinations. In Eq. (19) which has G parity negative, $K^{*+}K^- - \bar{K}^{*0}K^0$ has G parity positive. On the other hand, this combination has $I = 1, I_3 = 0$; hence, according to Table II, this combination is the one that creates the $b_1(1235)$, and thus Eq. (19) gives us a good combination. Since we do not want a π^0, at the end we choose the π^+ $(K^{*+}K^- - \bar{K}^{*0}K^0)$ combination, corresponding to $\pi^+ b_1^0$, then the b_1^0 decays to $\rho^0\eta$ (see Table VII of Ref. [27]), $\rho^0 \to \pi^+\pi^-$ and we have the desired final state.

We then select the hadronic component

$$|HI12\rangle = \pi^+(K^{*+}K^- - \bar{K}^{*0}K^0). \tag{21}$$

(3a) VP:

$$s\bar{d} \to \sum_i s\bar{q}_i q_i \bar{d} = \sum_i V_{3i}P_{i2} = (VP)_{32} = K^{*-}\pi^+ + \left(-\frac{\pi^0}{\sqrt{2}} + \frac{\eta}{\sqrt{3}}\right)\bar{K}^{*0} + \phi\bar{K}^0 \tag{22}$$

together with K^+.

(3b) PV:

$$s\bar{d} \to \sum_i s\bar{q}_i q_i \bar{d} = \sum_i P_{3i}V_{i2} = (PV)_{32} = K^-\rho^+ + \left(-\frac{\rho^0}{\sqrt{2}} + \frac{\omega}{\sqrt{2}}\right)\bar{K}^0 - \bar{K}^{*0}\frac{\eta}{\sqrt{3}} \tag{23}$$

together with K^+.

Unlike we had before, we do not make good combinations now for G parity, positive or negative. This is done when we consider the (4a) and (4b) combinations below.

(4a) VP:

$$u\bar{s} \to \sum_i u\bar{q}_i q_i \bar{s} = \sum_i V_{1i}P_{i3} = (VP)_{13} = \left(\frac{\rho^0}{\sqrt{2}} + \frac{w}{\sqrt{2}}\right)K^+ + \rho^+K^0 - K^{*+}\frac{\eta}{\sqrt{3}} \tag{24}$$

together with $\bar{K}^0$.

(4b) PV:

$$u\bar{s} \to \sum_i u\bar{q}_i q_i \bar{s} = \sum_i P_{1i}V_{i3} = (PV)_{13} = \left(\frac{\pi^0}{\sqrt{2}} + \frac{\eta}{\sqrt{3}}\right)K^{*+} + \pi^+K^{*0} + K^+\phi \tag{25}$$

together with $\bar{K}^0$.

We find now four combinations from (3a), (3b) and (4a) (4b), two with positive G parity and two with negative G parity. Those of negative G parity are

$$K^+(VP)_{32} - \bar{K}^0(PV)_{13} = \pi^+(K^{*-}K^+ - K^{*0}\bar{K}^0) - \frac{\pi^0}{\sqrt{2}}(\bar{K}^{*0}K^+ + K^{*+}\bar{K}^0) + \frac{\eta}{\sqrt{3}}(\bar{K}^{*0}K^+ - K^{*+}\bar{K}^0) \tag{26}$$

$$\bar{K}^0(VP)_{13} - K^+(PV)_{32} = \rho^+(K^0\bar{K}^0 - K^+K^-) + \sqrt{2}\rho^0(K^+\bar{K}^0) - \frac{\eta}{\sqrt{3}}(\bar{K}^0K^{*+} - \bar{K}^{*0}K^+) \tag{27}$$

and in Eq. (26) the π^0 term will not contribute. Similarly, the $K^0\bar{K}^0 - K^+K^-$ in Eq. (27) has $I = 1$ and corresponds to the a_0 with zero charge that decays to $\pi^0\eta$. Together with ρ^+, we would have $\pi^+\pi^0\pi^0\eta$ which is not the desired final state. Hence we have two good combinations.

$$|HI3213\rangle = \pi^+(K^{*-}K^+ - K^{*0}\bar{K}^0) + \frac{\eta}{\sqrt{3}}(\bar{K}^{*0}K^+ - K^{*+}\bar{K}^0) \tag{28}$$

$$|HI1332\rangle = \sqrt{2}\rho^0K^+\bar{K}^0 - \frac{\eta}{\sqrt{3}}(\bar{K}^0K^{*+} - \bar{K}^{*0}K^+). \tag{29}$$

Let us inspect these terms. The combination $K^{*-}K^+ - K^{*0}\bar{K}^0$ accompanying π^+ in Eq. (26) has G parity positive and is a mixture of $I = 0, 1$. According to Table II it could contribute to produce the $b_1(1235)$ or the $f_1(1285)$, but only the b_1 decays to $\rho\eta$; hence, we must project that state over the b_1. On the other hand, the combination $\bar{K}^{*0}K^+ - K^{*+}\bar{K}^0$ has $I = 1$, $I_3 = 1$, and with negative G parity it corresponds to the $a_1(1260)$. Finally, the $K^+\bar{K}^0$ accompanying ρ^0 in Eq. (29) has $I = 1$, $I_3 = 1$ and negative G parity and corresponds to the $a_0(980)$ resonance. As we can see, we have obtained terms that lead us to the $\pi^+\pi^+\pi^-\eta$ final state through the excitation of the $b_1(1235)$, $a_1(1260)$, and $a_0(980)$ resonances, which are well seen in the mass spectra of the experiment [16].

We have obtained four suitable states, $|HE3\rangle$, $|HI12\rangle$, $|HI3213\rangle$, and $|HI1332\rangle$. We shall give weights 1 to $|HE3\rangle$, α to $|HI3213\rangle$, β to $|HI1332\rangle$, and γ to $|HI12\rangle$, up to a global normalization factor C, and we get the contribution from one hadronization:

$$|H1\rangle \equiv C\Big[-\sqrt{\frac{2}{3}}\eta\rho^0\pi^+ + \frac{\eta}{\sqrt{3}}(1+\alpha+\beta)(\bar{K}^{*0}K^+ - K^{*+}\bar{K}^0) + \sqrt{2}\beta\rho^0 K^+\bar{K}^0 + \alpha\pi^+(K^{*-}K^+ - K^{*0}\bar{K}^0) - \gamma\pi^+(\bar{K}^{*0}K^0 - K^{*+}K^-)\Big]. \quad (30)$$

The first term in the former equation is a tree level contribution, then $\rho^0 \to \pi^+\pi^-$ and we shall have $\pi^+\pi^+\pi^-\eta$, the desired final state. The combinations with K, K^* will make transitions to other states to complete the $\pi^+\pi^+\pi^-\eta$ final state and we assume these transitions to be dominated by the corresponding resonances that they form within the chiral unitary approach.

In Refs. [22,27] the couplings of the resonances to the different components are given for the normalized states in the isospin basis. We must obtain the projection of the states obtained here on the isospin states of [22,27], which we do below.

(a) $\bar{K}^{*0}K^+ - K^{*+}\bar{K}^0$ has negative G parity and $I = 1$. It corresponds to the $a_1(1260)$ with $I_3 = 1$. Concretely, using the convention of Ref. [27], we have

$$|a_1, I_3 = 1\rangle = \frac{1}{\sqrt{2}}(\bar{K}^{*0}K^+ - K^{*+}\bar{K}^0).$$

Hence,

$$\langle a_1, I_3 = 1|\bar{K}^{*0}K^+ - K^{*+}\bar{K}^0\rangle = \sqrt{2}.$$

(b) $K^{*-}K^+ - K^{*0}\bar{K}^0$ and $\bar{K}^{*0}K^0 - K^{*+}K^-$ have both G parity positive and belong to the b_1 resonance. Once again, with the convention of Ref. [27] we have

$$|b_1, I_3 = 0\rangle = \frac{1}{\sqrt{2}}|\bar{K}^*K(I=1) + K^*\bar{K}(I=1)\rangle = \frac{1}{2}|\bar{K}^{*0}K^0 - K^{*-}K^+ - \bar{K}^{*+}K^- + K^{*0}\bar{K}^0\rangle.$$

Hence,

$$\langle b_1, I_3 = 0|K^{*-}K^+ - K^{*0}\bar{K}^0\rangle = -1,$$
$$\langle b_1, I_3 = 0|\bar{K}^{*0}K^0 - K^{*+}K^-\rangle = 1.$$

(c) $K^+\bar{K}^0$ is the $I_3 = 1$ component of $K\bar{K}$ that couples to $a_0(980)$. Hence

$$\langle a_0(980), I_3 = 1|K^+\bar{K}^0\rangle = 1.$$

The resonances formed will decay to different channels, a_1 to $\rho^0\pi^+$, b_1 to $\rho^0\eta$ and a_0 to $\pi^+\eta$ and we have the picture depicted in Fig. 3.

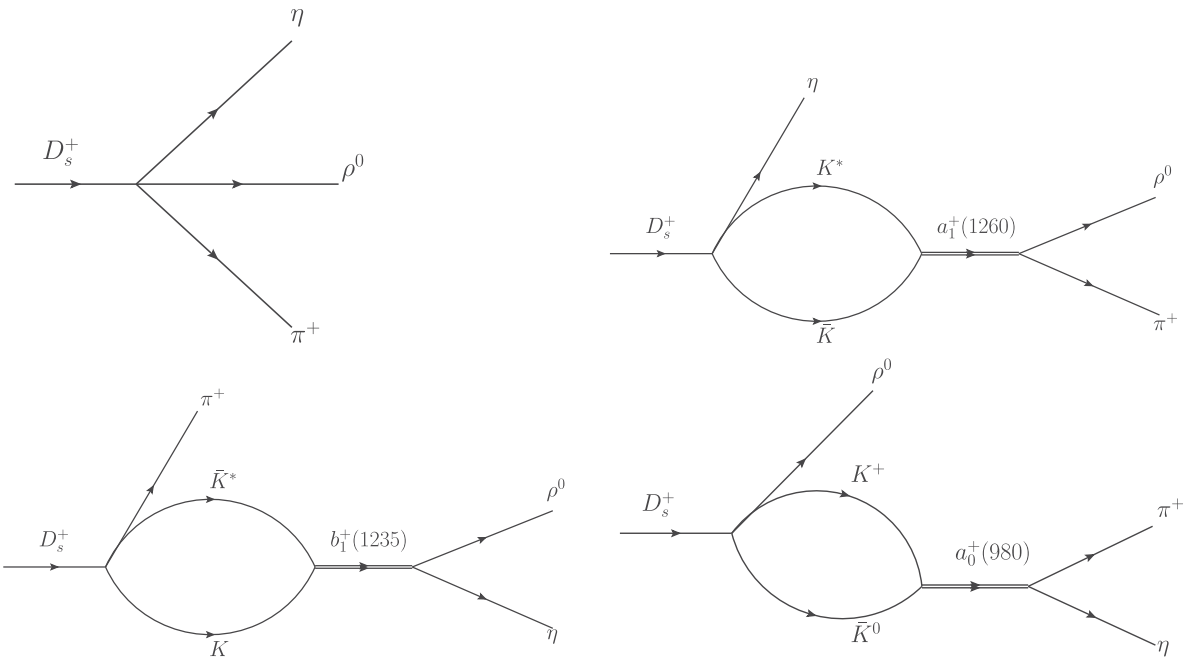

FIG. 3. Diagrams stemming from the hadronization of one $q\bar{q}$ pair.

We have established before the coupling of the $K^*\bar{K}$, $K\bar{K}$ channels to the a_1, b_1, and a_0 resonances. Now we must deal with their decays to $\rho\pi$, $\rho\eta$, and $\pi\eta$. We follow again Refs. [22,27].

(d) The $\rho\pi$ component for the $I_3 = 1$ state of the $a_1(1260)$ resonance is given considering the π, ρ isospin multiples $(-\pi^+, \pi^0, \pi^-)$, $(-\rho^+, \rho^0, \rho^-)$ by

$$|a_1, I_3 = 1\rangle = \left| -\frac{1}{\sqrt{2}}\rho^+\pi^0 + \frac{1}{\sqrt{2}}\rho^0\pi^+ \right\rangle$$

and we are interested only in the second component; hence, we have an overlap factor of $\frac{1}{\sqrt{2}}$.

(e) The $I_3 = 0$ $\rho\eta$ component of the b_1 is

$$|b_1, I_3 = 0\rangle = |\rho^0\eta\rangle;$$

the overlap factor is 1.

(f) The $I_3 = 0$, $I_3 = 1$ components of the $a_0(980)$ are

$$|a_0, I_3 = 0\rangle = |\pi^0\eta\rangle, \qquad |a_0, I_3 = 1\rangle = -|\pi^+\eta\rangle.$$

With all these weights calculated we obtain the following amplitude:

$$t_{H1}(\pi^+\rho^0\eta) = C\left[-\sqrt{\frac{2}{3}} + \frac{\eta}{\sqrt{3}}(1+\alpha+\beta)G_{K^*\bar{K}}(M_{\rm inv}(\rho^0\pi^+))\frac{g_{a_1,K^*\bar{K}}g_{a_1,\rho\pi}}{M^2_{\rm inv}(\rho^0\pi^+) - M^2_{a_1} + iM_{a_1}\Gamma_{a_1}}\right.$$
$$\left. - \sqrt{2}\beta G_{K\bar{K}}(M_{\rm inv}(\pi^+\eta))\frac{g_{a_0,K\bar{K}}g_{a_0,\pi\eta}}{M^2_{\rm inv}(\pi^+\eta) - M^2_{a_0} + iM_{a_0}\Gamma_{a_0}} - (\alpha+\gamma)G_{K^*\bar{K}}(M_{\rm inv}(\rho^0\eta))\frac{g_{b_1,K^*\bar{K}}g_{b_1,\rho\eta}}{M^2_{\rm inv}(\rho^0\eta) - M^2_{b_1} + iM_{b_1}\Gamma_{b_1}}\right] \tag{31}$$

where $G_{K^*\bar{K}}$, $G_{K\bar{K}}$ are the loop functions of two mesons which are regularized as in [27] for $G_{K^*\bar{K}}$ and with a cutoff method for $K\bar{K}$ as done in [4,31] with a cutoff off 600 MeV. The couplings of the a_1, b_1 resonances are taken from [27] and are shown in Table III, and the masses and widths are from the Particle Data Group (PDG) [32]. The $f_0(980)$ has a width of 10–100 MeV in the PDG and we take 70 MeV. One note is, however, mandatory here. The $a_0(980)$ usually is considered as a normal resonance. Yet, the high precision experiments where the $a_0(980)$ is seen lately [33,34] show a shape of the a_0 as a strong sharp peak in the $\pi^0\eta$ mass distribution, typical of a cusp, corresponding to a barely failed state, or virtual state. This is also the case in a large number of theoretical works [4,35–38]. In this case the couplings are not well defined. In fact, the couplings go to zero when one approaches a threshold as a consequence of the Weinberg compositeness condition [39–45]. This is so for one channel, but it also holds for all couplings when using coupled channels when one approaches one threshold [46,47]. Because of this we replace in Eq. (31).

$$\frac{g_{a_0,K\bar{K}}g_{a_0,\pi\eta}}{M^2_{\rm inv}(\pi^+\eta) - M^2_{a_0} + iM_{a_0}\Gamma_{a_0}} \to t^{I=1}_{K\bar{K},\pi\eta} \tag{32}$$

TABLE III. The couplings of the a_1 and b_1 states in the unit of MeV [27].

a_1		b_1	
$g_{\bar{K}^*K}$	$g_{\rho\pi}$	$g_{K^*\bar{K}}$	$g_{\rho\eta}$
$1872 - i1486$	$-3.795 + i2330$	$-3041 + i498$	$6172 - i75$

where $t^{I=1}_{K\bar{K},\pi\eta}$ is taken from the model of Ref. [4] using the chiral unitary approach with the $\pi\eta$ and $K\bar{K}$ channels.

D. Rescattering from the tree level $\eta\rho^0\pi^+$ component

In Eq. (31) we have the tree level $\eta\rho^0\pi^+$ term, and all the others come from one transition from the primary meson states generated in the weak process and one hadronization. In line with this extra final state interaction of the $K^*\bar{K}$, $K\bar{K}$ components, we address here the mechanisms of rescattering of the pairs of mesons in the tree level amplitude going to the same states. This leads to the diagrams shown in Fig. 4.

With the ingredients before it is easy to write this amplitude as

$$t_{\rm RES}(\rho^0\pi^+\eta)$$
$$= -C\sqrt{\frac{2}{3}}G_{\rho\pi}(M_{\rm inv}(\rho^0\pi^+))\frac{\frac{1}{\sqrt{2}}g_{a_1,\rho\pi}\frac{1}{\sqrt{2}}g_{a_1,\rho\pi}}{M^2_{\rm inv}(\rho^0\pi^+) - M^2_{a_1} + iM_{a_1}\Gamma_{a_1}}$$
$$- C\sqrt{\frac{2}{3}}G_{\rho\eta}(M_{\rm inv}(\rho^0\eta))\frac{g_{b_1,\rho\eta}g_{b_1,\rho\eta}}{M^2_{\rm inv}(\rho^0\eta) - M^2_{b_1} + iM_{b_1}\Gamma_{b_1}}$$
$$- C\sqrt{\frac{2}{3}}G_{\pi^+\eta}(M_{\rm inv}(\pi^+\eta))\frac{g_{a_0,\pi\eta}g_{a_0,\pi\eta}}{M^2_{\rm inv}(\pi\eta) - M^2_{a_0} + iM_{a_0}\Gamma_{a_0}} \tag{33}$$

where, once again, in the last term we shall make the replacement of Eq. (32).

There is still a bit extra work having to do with the ρ production and its decay to $\pi^+\pi^-$. First we must contract

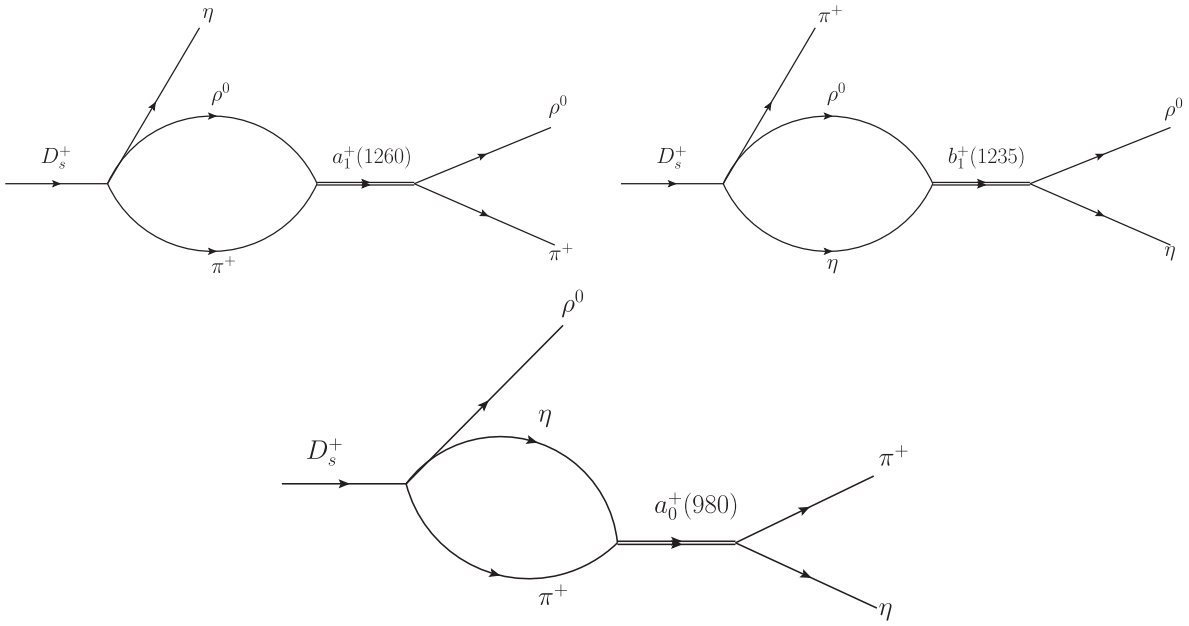

FIG. 4. Diagrams from the rescattering of pairs of mesons $\rho^0\pi^+\eta$ production.

the ρ^0 polarization vector with some momentum, since the D_s, η, π have no spin. Given that π and η are produced on the same footing, we could have $\epsilon_\mu(p_\pi + p_\eta)^\mu$, or $\epsilon_\mu P^\mu_{D_S}$, but since $p_D = p_\pi + p_\eta + p_\rho$ and $\epsilon_\mu P^\mu_{D_S} = 0$, these terms are equivalent and we take $\epsilon_\mu P^\mu_{D_S}$.

Next, when the ρ^0 decays to $\pi^+\pi^-$ there are two π^+ at the end, and one must symmetrize the amplitude. We shall have two diagrams, as depicted in Fig. 5.

Then, taking for instance the diagram of Fig. 5(a), we would have for the ρ propagator the sum over the ρ polarization.

$$\sum_{\text{pol}} P^\mu_D \epsilon_\mu \epsilon_\nu (p_4 - p_2)^\nu = P^\mu_D \left(-g_{\mu\nu} + \frac{q_\mu q_\nu}{m_{\rho^2}}\right)(p_4 - p_2)^\nu$$

with $q = p_2 + p_4$. Since $q(p_2 - p_4) = m_\pi^2 - m_\pi^2 = 0$ we have then $-p^\mu_D(p_4 - p_2)_\mu$ and the amplitudes become

$$t_\rho = -C\left[P_{D_s}\cdot(p_4 - p_2)\frac{1}{M^2_{\text{inv}}(\rho,a) - M^2_\rho + iM_\rho\Gamma_\rho}t^{(a)} + P_{D_s}\cdot(p_4 - p_3)\frac{1}{M^2_{\text{inv}}(\rho,b) - M^2_\rho + iM_\rho\Gamma_\rho}t^{(b)}\right] \quad (34)$$

where $t^{(a)}$ and $t^{(b)}$ are the amplitudes evaluated before with the momenta configuration of the diagrams of Figs. 5(a) and 5(b). $M^2_{\text{inv}}(\rho,a)$ and $M^2_{\text{inv}}(\rho,b)$ are p^2_ρ for the configurations of Figs. 5(a) and 5(b), respectively. We have omitted the $\rho\pi\pi$ coupling which is incorporated in the C global coefficient.

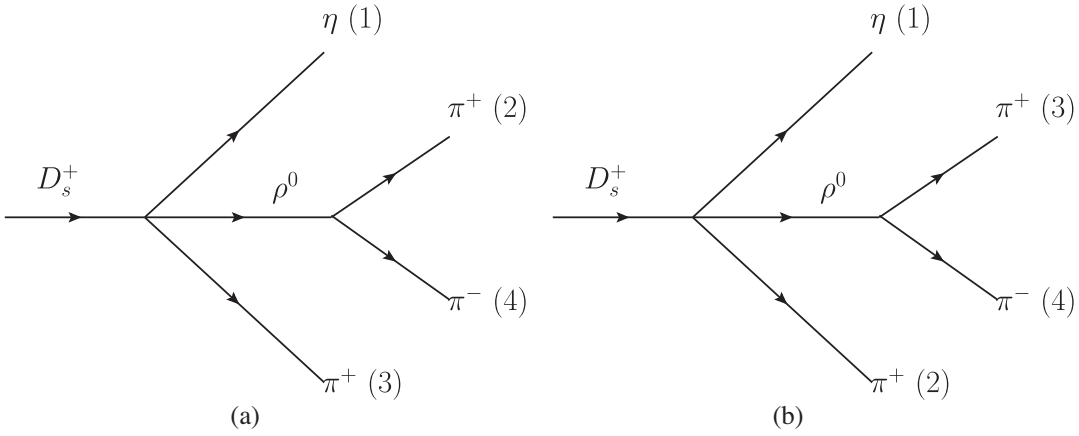

FIG. 5. Symmetrized amplitude with ρ decaying to two pions. (a) With the ρ^0 coming from pions (2) and (4); (b) with the ρ^0 coming from pions (3) and (4).

E. Two hadronizations with external emission: $f_0(980)$ contribution

In the $\pi^+\pi^-$ mass distribution of Ref. [16] one observes two structures, one for the ρ^0 and another one for the $f_0(980)$. So far neither the $f_0(980)$ nor the $a_0(980)$, with $I_3 = -1$ ($\pi^-\eta$), have appeared in our scheme. The reason lies in the fact that, up to now, we have only considered the mechanism with one hadronization providing VPP. Now we consider two hadronizations leading to four pseudoscalars $PPPP$. The corresponding external emission mechanism proceeds through the diagram given in Fig. 6 Since $\eta = \frac{1}{\sqrt{3}}(u\bar{u} + d\bar{d}) - \frac{1}{\sqrt{3}}s\bar{s}$ with the mixing of [30], the hadronization of the $\bar{d}u$ component can lead to $\pi^+\eta$ while the hadronization of $s\bar{s}$ can lead to $K\bar{K}$. We thus obtain $\pi^+\eta K\bar{K}$ which is not the desired final state. However, we can have the $K\bar{K} \to \pi^+\pi^-$ transition and then we get the $\pi^+\pi^+\pi^-\eta$ final state. In terms of resonances, $K\bar{K}$ coming from the $I = 0$ $s\bar{s}$ pairs can only give rise to the $f_0(980)$, the coupling to the $f_0(500)$ being very small. Hence, we find a mechanism for the production of this resonance, and we have two new diagrams, which are depicted in Fig. 7.

A caveat must be recalled at this point, since as discussed in [48], the coupling of W^+ to two pseudoscalars goes as the difference of energies of the two pseudoscalars which will vanish in the W^+ rest frame for two particles with the same mass. However, η and π have very different masses and the term survives.

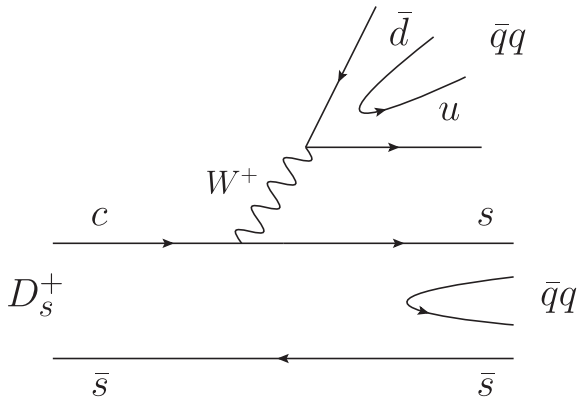

FIG. 6. Mechanism with two hadronizations producing four pseudoscalars.

After generating the two new mechanisms of Fig. 7, we can proceed further and take into account the final state interaction of the different components. This is depicted in Fig. 8. We should note that all the couplings here are of an S-wave nature, unlike the former diagrams that all contained a ρ^0 decaying to $\pi^+\pi^-$ in the P wave. A similar diagram to Fig. 8(b) could be done replacing the $f_0(980)$ by the ρ meson, but the extra loop with respect to the former diagrams, together with the factor $(p_4 - p_2)^0$ from Eq. (34), does not make it competitive in comparison with the mechanisms of Fig. 8 and we do not consider it here.

In the evaluation of the diagrams in Fig. 8 where the $f_0(980)$ is in the loop, we make some approximation to evaluate it. What makes the approximation good is the realization that the $f_0(980)$ in the loop is very far off shell. One interesting way to see it is to test how far one is from having a triangle singularity [49] which would place the $\pi\eta$ and $f_0(980)$ simultaneously on mass shell. For this we apply Eq. (18) of Ref. [50] and see that one is far from satisfying that condition, and since the $\pi\eta$ can be obviously on shell, from where the loop gets its maximum contribution, the $f_0(980)$ will be off shell. This allows us to factorize the $f_0(980)$ propagator in the loop. Taking as an example the loop in Fig. 8(f) we would have

$$D_{f_0} = \frac{1}{M^2_{\mathrm{inv}(\pi^-_{\mathrm{int}}\pi^+(2))} - M^2_{f_0} + iM_{f_0}\Gamma_{f_0}} \tag{35}$$

with π^-_{int}, the π^- inside the loop, where

$$\begin{aligned} M^2_{\mathrm{inv}}(\pi^-_{\mathrm{int}}\pi^+(2)) &= (w_{\pi^+(2)} + w_{\pi^-_{\mathrm{int}}})^2 - (\mathbf{p}_{\pi^+(2)} + \mathbf{p}_{\pi^-_{\mathrm{int}}})^2 \\ &= 2m^2_{\pi^+} + 2w_{\pi^+(2)}w_{\pi^-_{\mathrm{int}}} - 2\mathbf{p}_{\pi^+(2)}\mathbf{p}_{\pi^-_{\mathrm{int}}} \\ &\approx 2m^2_{\pi} + 2w_{\pi^+(2)}w_{\pi^-_{\mathrm{int}}} \end{aligned} \tag{36}$$

where in the last equation we have removed the $\mathbf{p}_{\pi^+(2)}\mathbf{p}_{\pi^-_{\mathrm{int}}}$ term, a sensible approximation if we evaluate Eq. (36) in the $\pi^-\eta$ rest frame when performing the $\mathbf{p}_{\pi^-_{\mathrm{int}}}$ integration in

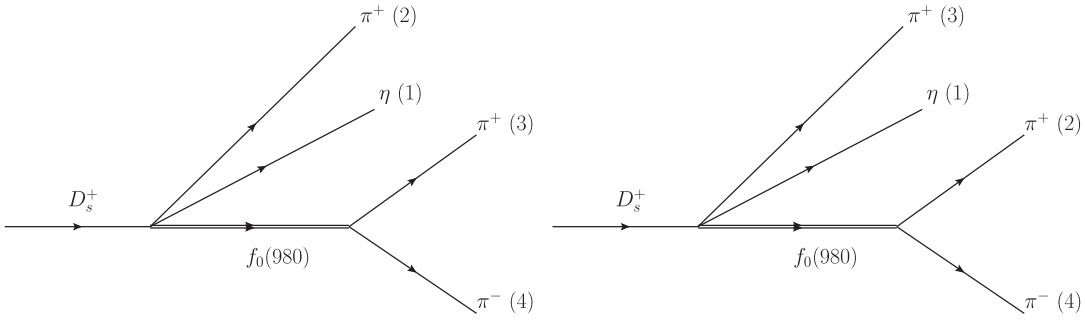

FIG. 7. Diagrams stemming from two hadronizations producing the $f_0(980)$ resonance.

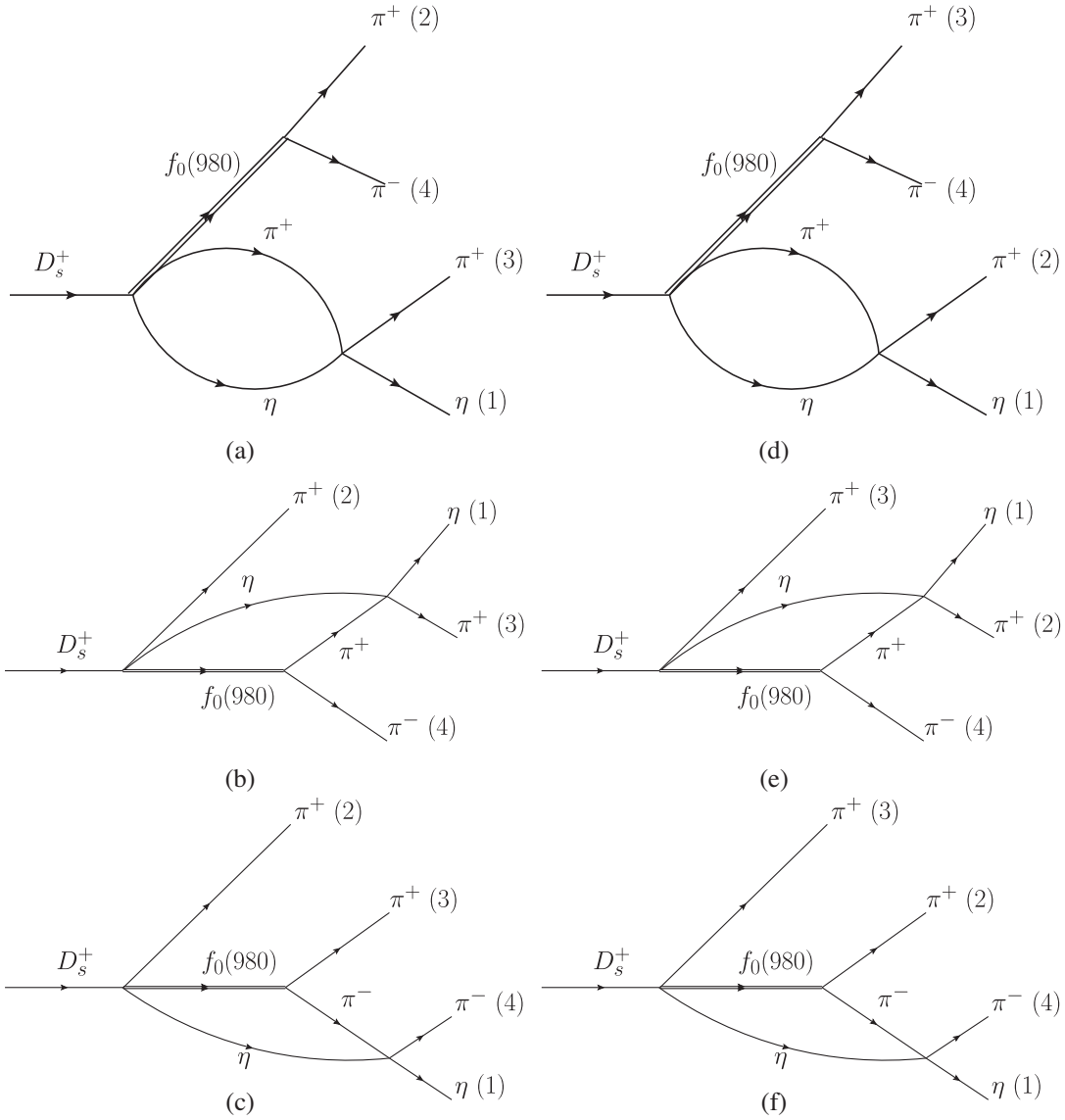

FIG. 8. Diagrams stemming from those of Fig. 7 after rescattering of two pseudoscalars. Diagrams (a) to (f) indicating different topologies of the interaction of mesons, see text.

the loop. Recalling that we get most of the contribution to the loop when $\pi^-_{\rm int}\eta$ are on shell we get

$$w_{\pi^-_{\rm int}} = \frac{M^2_{\rm inv}(\pi^-\eta) + m^2_{\pi^-} - m^2_\eta}{2M_{\rm inv}(\pi^-\eta)},$$
$$w_{\pi^+(2)} = \frac{p_{\pi^+(2)} \cdot (p_{\pi^-} + p_\eta)}{M_{\rm inv}(\pi^-\eta)}. \tag{37}$$

We multiply D_{f_0} by a factor $M_{f_0}\Gamma_{f_0}$ to have a dimensionless magnitude

$$\tilde{D}_{f_0} = M_{f_0}\Gamma_{f_0} D_{f_0}$$

and then we get for the diagrams of Figs. 7 and 8, $t_1(f_0)$ and $t_2(f_0)$ given by

$$t_1(f_0) = C\mu[\tilde{D}_{f_0}(M_{\rm inv}(\pi^+(3)\pi^-)) + \tilde{D}_{f_0}(M_{\rm inv}(\pi^+(2)\pi^-))] \tag{38}$$

$$t_2(f_0) = t_{2a}(f_0) + t_{2b}(f_0) + t_{2c}(f_0) + t_{2d}(f_0) + t_{2e}(f_0) + t_{2f}(f_0) \tag{39}$$

with

$$
\begin{aligned}
t_{2a}(f_0) &= C\mu\tilde{D}_{f_0}(M_{\rm inv}(\pi^+(2)\pi^-))G_{\pi\eta}(M_{\rm inv}(\pi^+(3)\eta))t_{\pi^+\eta,\pi^+\eta}(M_{\rm inv}(\pi^+(3)\eta))\\
t_{2d}(f_0) &= C\mu\tilde{D}_{f_0}(M_{\rm inv}(\pi^+(3)\pi^-))G_{\pi\eta}(M_{\rm inv}(\pi^+(2)\eta))t_{\pi^+\eta,\pi^+\eta}(M_{\rm inv}(\pi^+(2)\eta))\\
t_{2b}(f_0) &= C\mu\tilde{D}_{f_0}(M_{\rm inv}(\pi^-\pi^+_{\rm int}))G_{\pi\eta}(M_{\rm inv}(\pi^+(3)\eta))t_{\pi^+\eta,\pi^+\eta}(M_{\rm inv}(\pi^+(3)\eta))\\
t_{2c}(f_0) &= C\mu\tilde{D}_{f_0}(M_{\rm inv}(\pi^+(3)\pi^-_{\rm int}))G_{\pi\eta}(M_{\rm inv}(\pi^-\eta))t_{\pi^-\eta,\pi^-\eta}(M_{\rm inv}(\pi^-\eta))\\
t_{2e}(f_0) &= C\mu\tilde{D}_{f_0}(M_{\rm inv}(\pi^-\pi^+_{\rm int}))G_{\pi\eta}(M_{\rm inv}(\pi^+(2)\eta))t_{\pi^+\eta,\pi^+\eta}(M_{\rm inv}(\pi^+(2)\eta))\\
t_{2f}(f_0) &= C\mu\tilde{D}_{f_0}(M_{\rm inv}(\pi^+(2)\pi^-_{\rm int}))G_{\pi\eta}(M_{\rm inv}(\pi^-\eta))t_{\pi^-\eta,\pi^-\eta}(M_{\rm inv}(\pi^-\eta))
\end{aligned}
\tag{40}
$$

and summing all them we have

$$t_{f_0} = t_1(f_0) + t_2(f_0). \tag{41}$$

We should note that through the mechanism of Figs. 8(c) and 8(f) we obtain for the first time a signal for the $a_0^- \to \pi^-\eta$, which is also clearly visible in the $\pi^-\eta$ invariant mass of Ref. [16].

In Eqs. (38), (39),and (40) we used a Breit-Wigner distribution for the $f_0(980)$. By doing this we divert from generating it through the chiral unitary approach as we have done with the other resonances. There are technical reasons for it. The rescattering in the mechanisms of Fig. 8 are considerably more involved if one uses the chiral amplitudes. We justified before that the approximation done is fair for the rescattering mechanisms. Yet, we are using it also in Eq. (38) for the diagrams of Fig. 7 where the $f_0(980)$ is not in a loop. While using the chiral amplitude there is easy, the fact remains that the $f_0(980)$ comes with a small width when the $\eta\eta$ channels are explicitly considered and a cutoff of 600 MeV is used to get the appropriate mass [31]. A better reproduction is done using a more elaborate model, using the $\frac{N}{D}$ method with dispersion relations including a small genuine component [13,51]. Instead of using this elaborate formalism, and given the small contribution that we find (also in the experiment), we take the approximation of Eq. (35) with $\Gamma \approx 70$ MeV, within the 10–100 MeV range given by the PDG [32].

F. Two hadronizatons with internal emission

Now we produce directly four pseudoscalars through the mechanism of Fig. 9 The hadronization produces now

$$
\begin{aligned}
s\bar{d} \to (P^2)_{32} &= K^-\pi^+ - \bar{K}^0\frac{\pi^0}{\sqrt{2}}\\
u\bar{s} \to (P^2)_{13} &= \frac{\pi^0}{\sqrt{2}}K^+ + \pi^+K^0
\end{aligned}
\tag{42}
$$

and thus, we have together

$$K^-K^+\pi^+\frac{\pi^0}{\sqrt{2}} + K^-\pi^+\pi^+K^0 - \bar{K}^0\frac{\pi^0}{\sqrt{2}}\frac{\pi^0}{\sqrt{2}}K^+ - \bar{K}^0\frac{\pi^0}{\sqrt{2}}\pi^+K^0$$

which indicates that only the second term can contribute to our process through $K^-K^0 \to a_0^- \to \pi^-\eta$ via the loop shown in Fig. 10. The amplitude for this process will be written as

$$t_{\rm DIE} = C\nu G_{K\bar{K}}(M_{\rm inv}(\pi^-\eta))t_{\pi^-\eta,K^0K^-} \tag{43}$$

where $t_{\pi^-\eta,K^0K^-} \equiv t^{I=1}_{\pi\eta,\pi\eta}$.

Coming from a double hadronization and internal emission, the term should be smaller than former ones and we refrain from studying further interactions. We

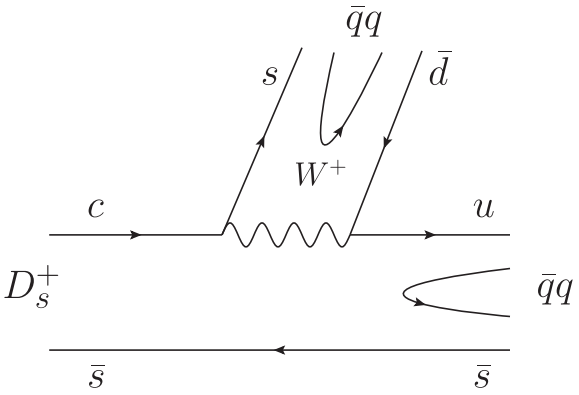

FIG. 9. Diagram for internal emission with two hadronizations.

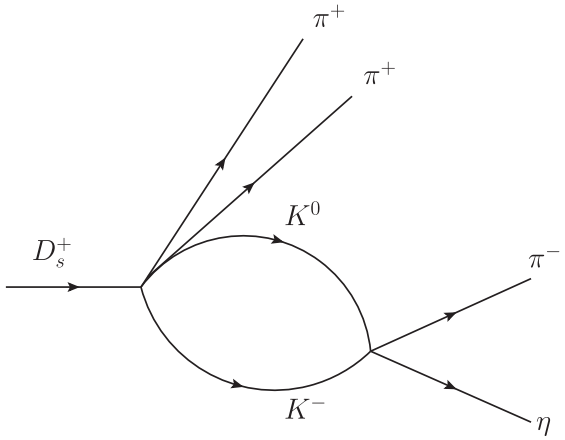

FIG. 10. Mechanism contributing to the $\pi^+\pi^+\pi^-\eta$ production stemming from the diagram of Fig. 9.

collect all the amplitudes from t_{H1}, $t_{\rm RES}$, properly symmetrized and accounting for ρ decay as shown in Eq. (34) plus t_{f_0} and $t_{\rm DIE}$ to construct the full amplitude, t. We have five parameters in addition to the global normalization constant C, which will be fitted to the data. In the following section we show how to evaluate the different cross sections.

All the final state interaction is done by allowing pairs of particles to interact, which is the most common approach taken in the literature. Yet, one could also have interactions of trios and four-body. We are assuming them to be small compared to the two body interactions that generate resonances. While one cannot rule out some contributions that could change the distributions a bit, we can argue that their contribution should be small. Indeed, as a general rule any extra hadron interaction weakens the contribution of a mechanism, unless the interaction is strong enough to produce a resonance. We can thus look at possible three-body resonances in the range covered by the D^+ decay. In the review paper [52] a complication of three-meson resonance states has been reported (see Table I of [52]) and the only one that could play a role here as the $\pi(1300)$ state which is obtained in [53] from the $\pi\pi\eta$ and $\pi K\bar{K}$ coupled channels. Yet, if one observes the $\pi^+\pi^-\pi^-\eta$ mass distribution in the experiment [16] there is no visible trace of this resonance, up to one deviation point, which is compatible with a statistical fluctuation.

III. EVALUATION OF THE DIFFERENTIAL CROSS SECTION

The width for the D_s decay into $\pi^+\pi^+\pi^-\eta$ is given by

$$\Gamma=\frac{1}{2M_{D_s}}\frac{1}{2}\int\frac{d^3p_\eta}{(2\pi)^3}\frac{1}{2E_\eta}\int\frac{d^3p_{\pi^+}}{(2\pi)^3}\frac{1}{2E_{\pi^+}}\int\frac{d^3p'_{\pi^+}}{(2\pi)^3}\frac{1}{2E'_{\pi^+}}\times\int\frac{d^3p_{\pi^-}}{(2\pi)^3}\frac{1}{2E_{\pi^-}}(2\pi)^4\delta^{(4)}(P-p_\eta-p_{\pi^+}-p'_{\pi^+}-p_{\pi^-})|t|^2, \tag{44}$$

with the factor $1/2$ since we have a symmetrized amplitude with respect to the two π^+. We kill the p_{π^-} integration with the $\delta^3()$ function, which gives us

$$\mathbf{p}_{\pi^-}=-(\mathbf{p}_\eta+\mathbf{p}_{\pi^+}+\mathbf{p}'_{\pi^+}).$$

We introduce the variable

$$\mathbf{P}_\pi=\mathbf{p}_{\pi^+}+\mathbf{p}'_{\pi^+},$$
$$\mathbf{q}_\pi=\mathbf{p}_{\pi^+}-\mathbf{p}'_{\pi^+},$$

which gives us

$$\Gamma=\frac{1}{2M_{D_s}}\frac{1}{2}\frac{1}{2}\int\frac{d^3p_\eta}{(2\pi)^3}\frac{1}{2E_\eta}\int\frac{d^3P_\pi}{(2\pi)^3}\times\int\frac{d^3q}{(2\pi)^3}\frac{1}{2E_{\pi^+}}\frac{1}{2E'_{\pi^+}}\frac{1}{2E_{\pi^-}}(2\pi)\delta(M_{D_s}-E_\eta-E_{\pi^+}-E'_{\pi^+}-\sqrt{m^2_{\pi^-}+(\mathbf{P}_\pi+\mathbf{p}_\eta)^2})|t|^2. \tag{45}$$

The $\delta()$ condition allows us to obtain $\cos\theta$ between $\mathbf{P}_\pi$ and $\mathbf{p}_\eta$ as a function of the other variables and we choose η in the z direction. We find

$$\cos\theta\equiv A=\frac{1}{2P_\pi p_\eta}[(M_{D_s}-E_\eta-E_{\pi^+}-E'_{\pi^+})^2-m^2_{\pi^-}-\mathbf{P}^2_\pi-\mathbf{p}^2_\eta]$$

but we must demand that $|\cos\theta|\leq 1$ and we implement the factor in the integrand

$$\theta(1-A^2)\theta(M_{D_s}-E_\eta-E_{\pi^+}-E'_{\pi^+}).$$

Then the width is finally written as

$$\Gamma=\frac{1}{8M_{D_s}}\frac{1}{\pi}\int p^2_\eta dp_\eta\frac{1}{2E_\eta}\int\frac{P^2_\pi dP_\pi d\phi}{(2\pi)^3}\times\int\frac{d^3q}{(2\pi)^3}\frac{1}{2E_{\pi^+}}\frac{1}{2E'_{\pi^+}}\frac{1}{2P_\pi p_\eta}|t|^2\theta(1-A^2)\times\theta(M_{D_s}-E_\eta-E_{\pi^+}-E'_{\pi^+}), \tag{46}$$

and we take

$$\mathbf{p}_\eta=p_\eta\begin{pmatrix}0\\0\\1\end{pmatrix};\qquad\mathbf{P}_\pi=P_\pi\begin{pmatrix}\sin\theta\cos\phi\\\sin\theta\sin\phi\\\cos\theta\end{pmatrix},$$
$$(\cos\theta=A,\sin\theta=\sqrt{1-A^2}). \tag{47}$$

However, it is convenient to define $\mathbf{q}$ with respect to $\mathbf{P}_\pi$ for integration purposes since it allows $A\equiv\cos\theta$ to be expressed in terms of the integration variables, as $\mathbf{p}_{\pi^+}=\frac{1}{2}(\mathbf{P}_\pi+\mathbf{q})$, $\mathbf{p}'_{\pi^+}=\frac{1}{2}(\mathbf{P}_\pi-\mathbf{q})$. Hence we define $\tilde{\mathbf{q}}$ related to $\mathbf{P}_\pi$ as the z axis as

$$\tilde{\mathbf{q}}=q\begin{pmatrix}\sin\tilde{\theta}_q\cos\tilde{\phi}_q\\\sin\tilde{\theta}_q\sin\tilde{\phi}_q\\\cos\tilde{\theta}_q\end{pmatrix},$$

and to write it in the D_s rest frame with $\mathbf{p}_\eta$ in the z direction, we make two rotations and find $\mathbf{q}=R\tilde{\mathbf{q}}$ with

$$R = R_\phi R_\theta = \begin{pmatrix} \cos\phi & -\sin\phi & 0 \\ \sin\phi & \cos\phi & 0 \\ 0 & 0 & 1 \end{pmatrix} \begin{pmatrix} \cos\theta & 0 & \sin\theta \\ 0 & 1 & 0 \\ -\sin\theta & 0 & \cos\theta \end{pmatrix} = \begin{pmatrix} \cos\phi\cos\theta & -\sin\phi & \cos\phi\sin\theta \\ \sin\phi\cos\theta & \cos\phi & \sin\phi\sin\theta \\ -\sin\theta & 0 & \cos\theta \end{pmatrix}.$$

With this choice: $E_{\pi^+} + E'_{\pi^+}$ entering the definition of $A \equiv \cos\theta$ is given by

$$\begin{aligned} E_{\pi^+} + E'_{\pi^+} &= \sqrt{m_\pi^2 + \frac{1}{4}(\mathbf{P}_\pi + \mathbf{q})^2} + \sqrt{m_\pi^2 + \frac{1}{4}(\mathbf{P}_\pi - \mathbf{q})^2} \\ &= \sqrt{m_\pi^2 + \frac{1}{4}P_\pi^2 + \frac{1}{4}q^2 + \frac{1}{2}P_\pi q\cos\tilde{\theta}_q} \\ &\quad + \sqrt{m_\pi^2 + \frac{1}{4}P_\pi^2 + \frac{1}{4}q^2 - \frac{1}{2}P_\pi q\cos\tilde{\theta}_q}. \end{aligned}$$

With these new variables and using $p_\eta \mathrm{d}p_\eta = E_\eta \mathrm{d}E_\eta$ we can write the width as

$$\Gamma = \frac{1}{8M_{D_s}}\frac{1}{4\pi}\int \mathrm{d}E_\eta \int \frac{P_\pi \mathrm{d}P_\pi \mathrm{d}\phi}{(2\pi)^3}\int \frac{q^2 \mathrm{d}q \mathrm{d}\cos\tilde{\theta}_q \mathrm{d}\tilde{\phi}_q}{(2\pi)^3} \times \frac{1}{2E_{\pi^+}}\frac{1}{2E'_{\pi^+}}|t|^2\theta(1-A^2)\theta(M_{D_s} - E_\eta - E_{\pi^+} - E'_{\pi^+}). \tag{48}$$

The choice of variable was done such that we can evaluate the integral and mass distributions using Monte Carlo integration. We have six integration variables. Random values within limits are chosen for all of them and the events are weighed by the integrand, and the $\theta()$ functions in Eq. (48) determine the phase space. With these variables, we construct all the momenta of the four final particles, which allows us to calculate the six invariant mass distributions. We accumulate the weighed events in boxes of mass distributions of 25 MeV, like in the experiment, and with $\sim 10^7$ generated events we get very accurate numerical mass distributions.

IV. RESULTS

First we go to Eq. (48) and substitute $t = 1$ in order to obtain the mass distributions with pure phase space. The results are shown, with the mass distributions, normalized to the data, in Fig. 11. In the same figure we also show the results obtained at the tree level of t_{H1}, with the $\pi^+\rho\eta$ amplitude of Eq. (31) keeping only the term $\sqrt{\frac{2}{3}}$, considering the ρ decay as shown in Eq. (34).

What we see in the figure is that in the case of phase space, one is obviously missing all the different structures which are visible in the experimental data: the ρ^0 peak in the $M(\pi^+\pi^-)$ distribution, the $a_0^+(980)$ in the $M(\pi^+\eta)$ distribution, and the $f_0(980)$ in the $M(\pi^+\pi^-)$ distribution. The effect of the $a_1(1260)$ (very wide) and of the b_1 are not so clear. Yet, the phase space alone fairly reproduces the gross features of the mass distribution, except for the case of the $M(\pi^+\pi^-)$, where the prominent peak of the ρ is obviously absent.

In the same figure we have the contribution of the $\pi^+\rho^0\eta$ term alone at the tree level. We can now see that the $M(\pi^+\pi^-)$ distribution is fairly well reproduced with its prominent ρ peak. It is very interesting to note that this term alone also creates a broad bump in $M(\pi^+\pi^-)$ at low energies around 0.5 GeV. This is particularly relevant since one could intuitively think that this bump comes from the production of the $f_0(500)$, as is seen in many other experiments. But we saw that in our exhaustive list of mechanisms of the reaction the $f_0(500)$ was never produced. We obtained the $f_0(980)$ via the $K\bar{K}$ coupling, but the $f_0(500)$ is well known to couple extremely weakly to this component [22–25]. Instead, we see that without producing this resonance, the ρ term gives rise to this wide bump. This is a consequence of the fact that we have two π^+ and if one $\pi^+\pi^-$ pair creates the ρ^0, the other $\pi^+\pi^-$ pair creates a different structure, which in this case is a $M(\pi^+\pi^-)$ distribution mimicking the $f_0(500)$ distribution. The other interesting thing is that now this term has widely distorted the other mass distributions, creating peaks or bumps that are in sheer contradiction with the experiment. These extra peaks are also well known in mass distributions when one has many particles in the final state, and are called replicas or reflections in other channels of genuine resonances of one channel. The fact that we also have two π^+ certainly has something to say. What is clear after we introduce the important $\rho^0\pi^+\eta$ term of tree level, is that we need other contributions to describe the experimental data.

Our formalism comes from the systematic consideration of all possible mechanisms and we saw that they indeed produced the a_0^+, a_0^-, a_1^+, b_1^+, $f_0(980)$ resonances through rescattering of meson-meson components that were produced in a first step of the weak reaction upon the hadronization of one or two pairs of $q\bar{q}$. These transitions had no freedom since for them we took the amplitudes generated by the chiral unitary approach. At the end of the large amount of terms collected we had, up to a global normalization constant, five free parameters, We should emphasize that the filter of G-parity negative eliminated terms, and it was linear contributions of states produced in different mechanisms that at the end gave us the desired $\pi^+\pi^+\pi^-\eta$ in the final state. Also, some terms of G-parity negative were shown not to lead to the desired final state and were eliminated. At the end, it is not easy to trace back the relative size of these parameters which have been assumed to be real as it would be the case in a quark model evaluation of the weak process plus the subsequent hadronization. Note, however, that the G functions and t_i

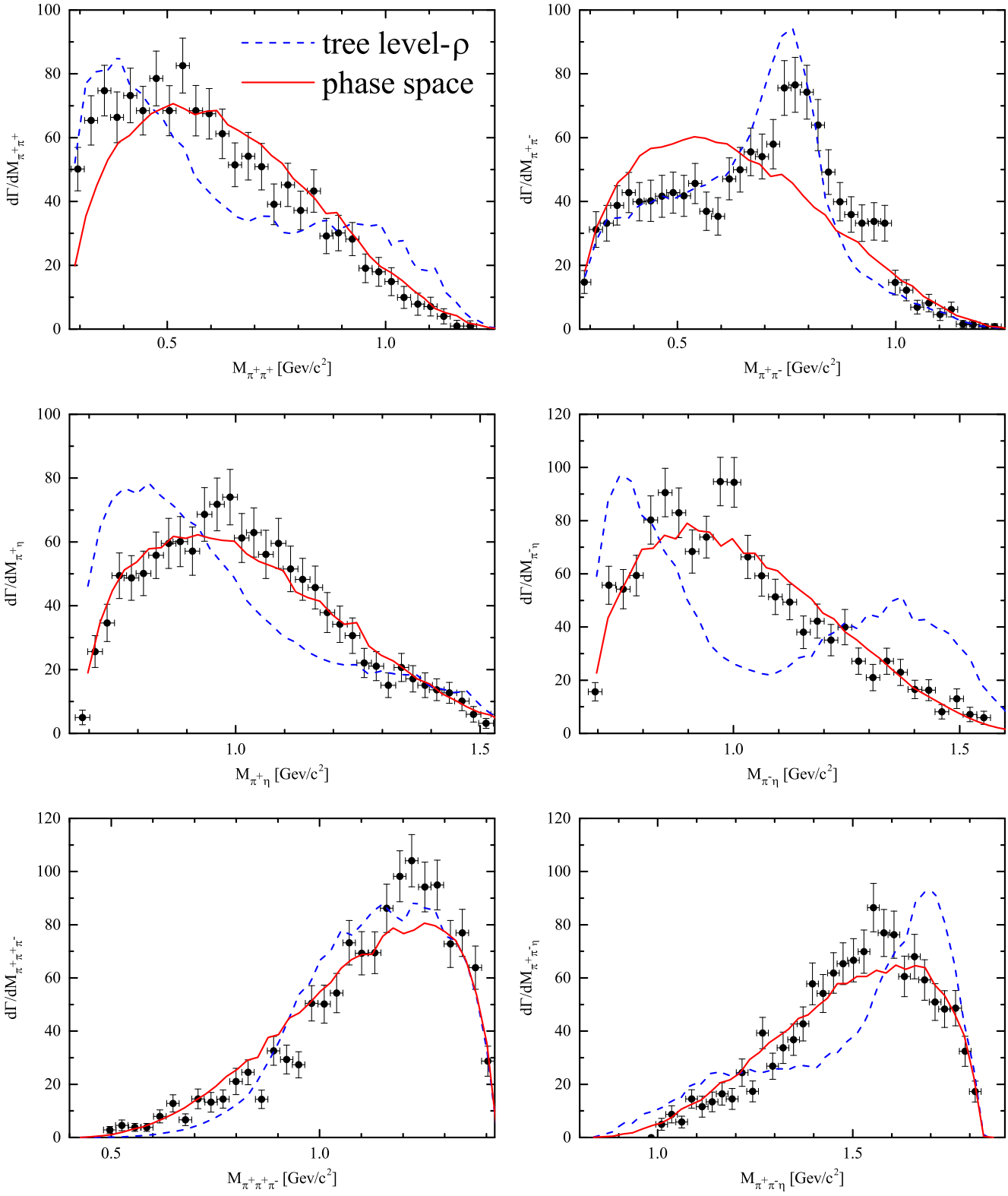

FIG. 11. Phase space and the tree level of ρ.

matrices are complex; therefore, our final amplitudes are complex and there are inevitably large interferences.

We, thus, conduct a best fit to all the six mass distributions and obtain the results that we show in Fig. 12. The improvement over the mass distributions of the tree level $\rho^0\pi^+\eta$ term is remarkable. The $\chi^2_{\text{d.o.f.}}$ is 1.77, which can be considered acceptable. The p value of the global fit is $p \approx 0.11$ indicating that the fit is significant. The values obtained for the parameters are shown below

$$\alpha = 4.2, \qquad \beta = 2.9, \qquad \gamma = -3.9,$$
$$\mu = -31.2, \qquad \nu = 39.1. \tag{49}$$

Inspection of the figures shows rather featureless $M(\pi^+\pi^+)$ distributions as also seen in the experiment. The $M(\pi^+\pi^-)$ distribution shows clearly the ρ^0 and the $f_0(980)$ peaks. Also, the low energy bump of the mass distribution is well reproduced which, as we discussed above, should not be associated to $f_0(500)$ excitation. In the same $M(\pi^+\pi^-)$ distribution we also see now a peak for the $f_0(980)$. The $M(\pi^+\eta)$ distribution comes out fairly well and a peak is seen corresponding to the $a_0^+(980)$ resonance. The resulting $M(\pi^+\pi^+\pi^-)$ and $M(\pi^+\pi^-\eta)$ distributions are also in good agreement with the corresponding experimental ones. The $M(\pi^-\eta)$ distribution shows a clear peak for the $a_0^-(980)$, as in the experiment, and the low and high energy parts of the spectrum are also well reproduced. There is a discrepancy with the data in a peak around 0.85 GeV that we cannot reproduce and do not know its dynamical origin.

Next, apart from the ρ already addressed, we would like to discuss the contribution of the different resonances to the six invariant mass distributions in Fig. 13. One must look at this information with care because there are interferences among the different amplitudes, but it gives an idea on how they appear in the process. For this we take the fitted amplitude and isolate the different terms of this amplitude where each resonance appears, and with only these terms we see the individual contributions to the mass distributions. As can be immediately appreciated, the dominant contribution comes from a_0^+. However, one should note that, as seen in Eq. (31) where the a_0^+ appears, it goes together with the ρ^0. Then it is not surprising to see a structure in $M(\pi^+\pi^-)$ and $M(\pi^-\eta)$ similar to the one produced by the ρ term alone shown in Fig. 11. In our formalism we cannot disentangle that structure. The a_0^- excitation has also a relatively large strength. The a_1^+ shows a clear peak around 1260 MeV, in the $\pi^+\pi^+\pi^-$, as it should be. Curiously, our mechanisms allow the excitation of the b_1^+, but the strength obtained is practically negligible. One should note that in the experimental analysis that the $b_1\pi$ mode was also not reported. Finally, we also show the contribution of the case where we set $\alpha = \beta = \gamma = \mu = \nu = 0$. The remaining amplitude still contains the tree level $\pi^+\rho^0\eta$ of Eq. (31) plus the term $\frac{\eta}{\sqrt{3}} G_{K^*\bar{K}} \frac{g_{a_1,K^*K} g_{a_1,\rho\pi}}{M^2_{\text{inv}}(\rho^0\pi^+) - m^2_{a_1} + i m_{a_1}\Gamma_{a_1}}$ with $\rho^0\pi^+\eta$ in the final state. Hence, we see the ρ peak again in the $M(\pi^+\pi^-)$ distribution. Not surprisingly, the a_1 term contribution, which contains this term in the way we calculate, still shows a peak for the ρ. The other thing that we observe is that the interferences are important in order to give the final structures.

The exercise done here shows the complexity of the current problem, and why a standard fit summing Breit-Wigner structures for resonant excitation, as it is usually done in experimental analysis, must be taken with care. While we get the different important modes reported in [16], the a_1 signal, which is the dominant one in [16], is relevant in our study but not dominant, and the fit fraction of 12.7% reported in [16] for the $f_0(500)\pi^+$ mode is absent in our study. However, we could find the origin of the seeming $f_0(500)$ peak in $M(\pi^+\pi^-)$, because one has two $\pi^+\pi^-$ at the end: one $\pi^+\pi^-$ pair producing the ρ and the other giving rise to this bump.

We would like to add to this discussion the comment that in the experimental analysis of this reaction, 10 fit fractions and nine phases where considered as free parameters. We only have five parameters and a global normalization. The fact that the resonances studied were all dynamically generated, except for the ρ, from pseudoscalar-pseudoscalar or pseudoscalar-vector interactions, and that we could relate to the different weak decay modes the production of these meson-meson components, established constraints on the relative production of these resonances. In addition, we also benefitted from having couplings of resonances to the different meson channels, provided by the chiral unitary approach, such that, at the end, we had a significantly smaller freedom to fit the data, in spite of which we could get a fair reproduction of them.

To finalize this section we address here the issue of the errors in the parameters and uncertainties in our fit. In the Minuit fits that we perform we obtain the value of the parameters of the best fit and their errors. The errors for the parameters obtained from this source are large, at the order of the value of the parameters themselves. This might indicate that we have large uncertainties in our fit, but, as normally happens when one has a relative number of parameters, this could be an indication that there are correlations between the parameters, and a large change in one of them can be compensated by changes in the other parameters. This is, indeed, the case here as we show with the following exercise. One way which is practical to show these correlations and establish the uncertainties in the fit is the following [54–60]: we generate random numbers for each data point within the error band of the point, and with these new data points and the same errors we conduct a fit. We repeat the procedure generating a new set of random points and performing a new fit. This is done a relatively large number of times and for each of them we plot the

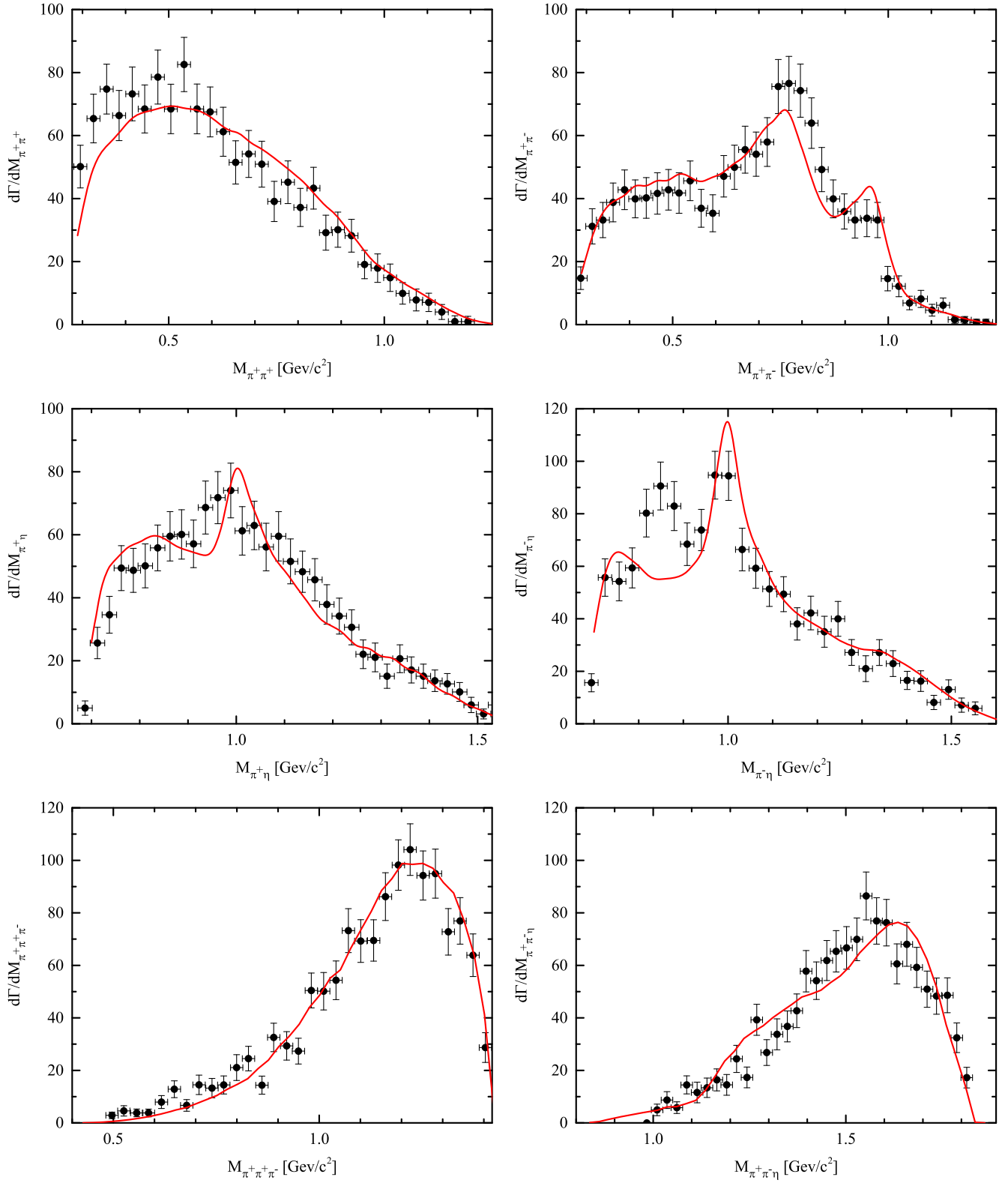

FIG. 12. The experimental data are from BESIII [16]. The red lines show the different mass distributions of $\pi^+\pi^+$, $\pi^+\pi^-$, $\pi^+\eta$, $\pi^-\eta$, $\pi^+\pi^+\pi^-$, and $\pi^+\pi^-\eta$, individually.

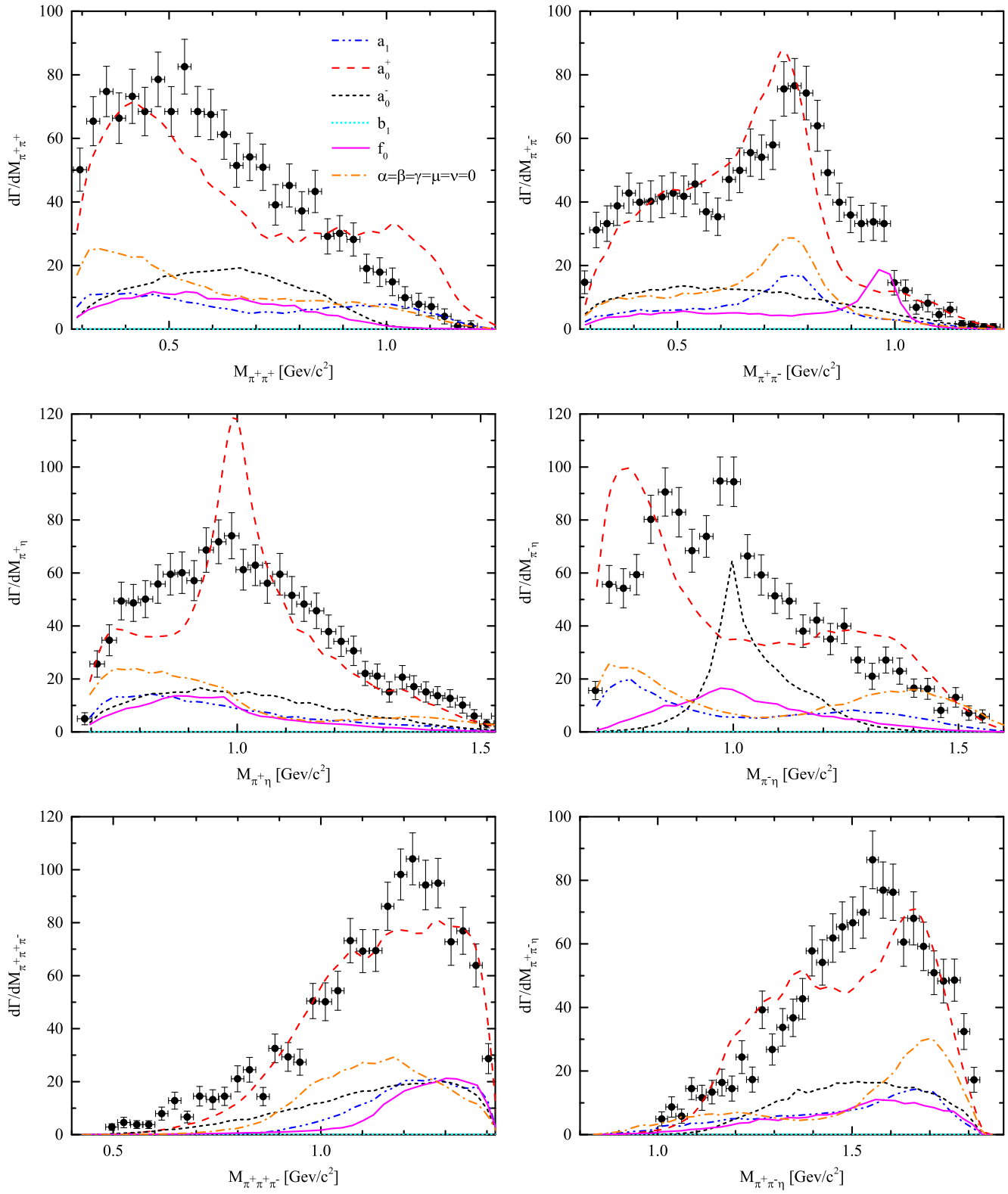

FIG. 13. The contributions of a_1, a_0^+, a_0^-, b_1, f_0, and external emission, respectively.

results for each distribution. At the end of the procedure we have a band of values from where one can conclude the goodness of the fit. For practical reasons we repeat the procedure 20 times, which we find sufficient to show the uncertainties of our fit. This method, known in statistics as the resampling-bootstrap method, produces correctly the covariance matrix and, although computing is costly since it involves many fits, is becoming increasingly more used,

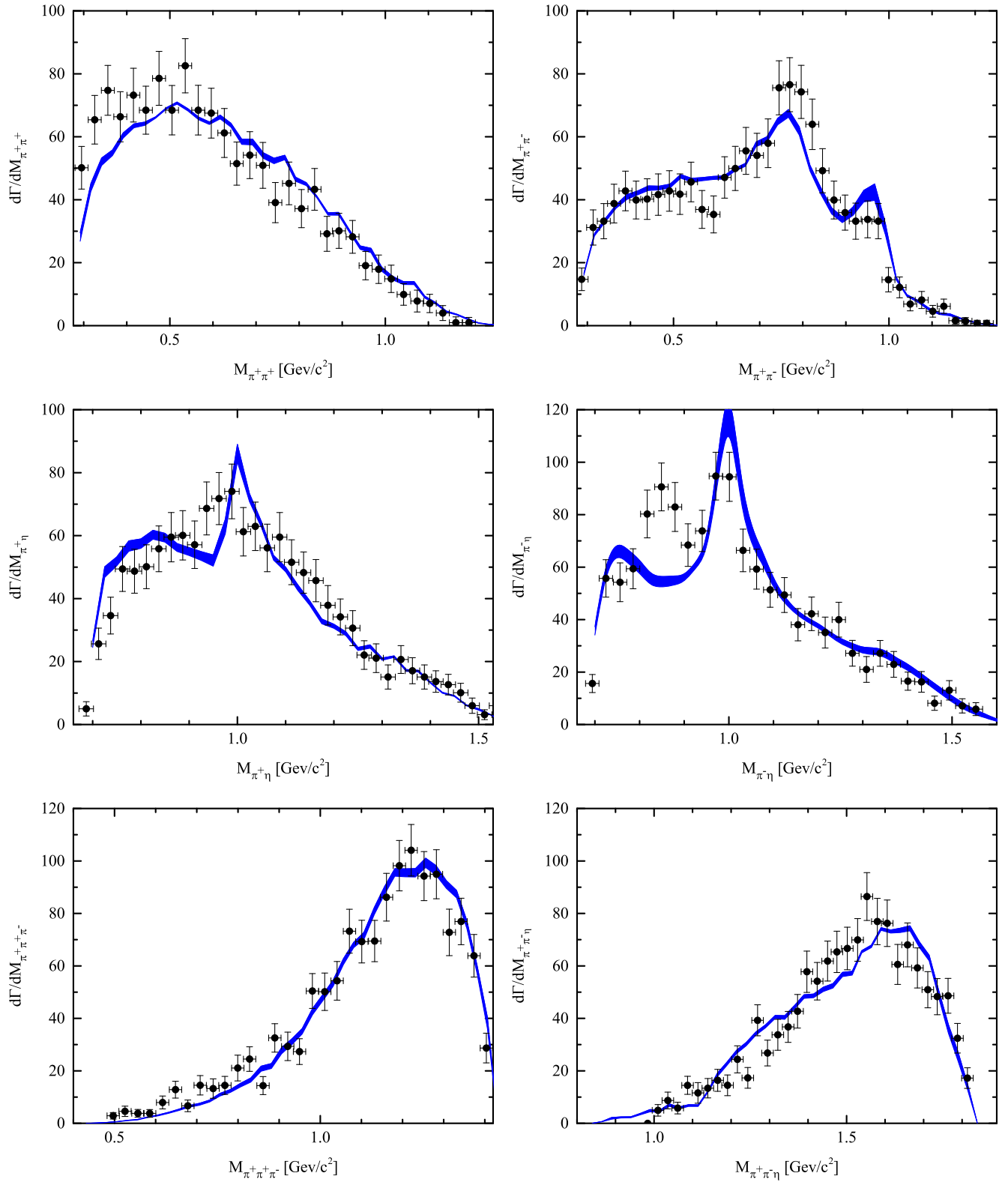

FIG. 14. Theoretical error bands. The blue area corresponds to the error band related to the different mass distributions, namely, $\pi^+\pi^+$, $\pi^+\pi^-$, $\pi^+\eta$, $\pi^-\eta$, $\pi^+\pi^+\pi^-$. The experimental data are from BESIII [16].

with increased computing capacities, given its technical simplicity.

The bands obtained are shown in Fig. 14.[1] It is surprising to see that the bands are so narrow, indicating small uncertainties in the fit results. And we, indeed, see that the parameters are different for each fit, indicating the strong correlations that one has. This also tell us that the value of the parameters obtained have to be taken with care. The fit to the data does not allow one to determine them individually with great precision, but the combination of terms can lead to a precise fit to the data. Another reading of these results is that, given the small dispersion of the mass distributions from all the random fits, any persistent discrepancy with the data has to find an explanation beyond the theoretical framework that we have performed.

V. CONCLUSIONS

We have made a theoretical study of the $D_s^+ \to \pi^+\pi^+\pi^-\eta$ reaction taking into account the final state interaction of pairs of mesons. The pairs are not necessarily those of the final state, because we consider coupled channels, and it is possible to produce some mesons in a first step which lead to the final $\pi^+\pi^+\pi^-\eta$ state making transitions with the strong interaction. The problem is complicated because of the many possible intermediate states but we followed a systematic study in which we looked at the weak decay processes, Cabibbo favored, that stemmed from $D_s \to$ quarks with external and internal emission. Then we allowed for one or two hadronizations of $q\bar{q}$ pairs to obtain mesons. Even then, there were many possible channels, but the filter of G parity of these states reduced considerably the number of possible combinations. Also, some of these were shown to be unable to produce the $\pi^+\pi^+\pi^-\eta$ final state after rescattering. This allowed us to have a manageable amount of terms at the end, with only a few parameters correlating them. The transition t matrices needed to go from these selected channels to the final state are all taken from the chiral unitary approach. At the end we have some amplitudes which interfere among them, from where we can get the six mass distributions and compare them with the experiment. The amplitudes that we obtain through final state interaction generate scalar and axial vector resonances, $a_0(980)$, $f_0(980)$, $a_1(1260)$, and $b_1(1235)$, which are visible in the experimental mass distributions, except for the $b_1(1235)$ which also comes with negligible strength in our study.

We obtain an acceptable fit to the six mass distributions with considerably less freedom in the parameter space than in the experimental analysis, which should be considered as a support for the amplitudes that we obtain using the chiral unitary approach, where the low lying scalar mesons are generated from the pseudoscalar-pseudoscalar interaction and the axial vector resonances from the pseudoscalar-vector interaction. The relevant modes obtained from a fit to the data with a sum of Breit-Wigner structures in the experimental analysis were also found in our study, but we had less strength for the dominant $a_1(1260)$ mode, although we noted that there are large interferences of the amplitudes and one must look with caution at the meaning of a fit fraction. An interesting feature is that the $f_0(500)$ was not produced in our approach, but the broad bump seen in the $M(\pi^+\pi^-)$ mass distribution around 500 MeV came as a consequence of having two π^+ in the final state, from the "wrong" $\pi^+\pi^-$ pair when the "good" $\pi^+\pi^-$ pair produced the ρ^0.

In these mass distributions we could clearly see peaks for the ρ^0, a_0^+, a_0^-, $f_0(980)$ and $a_1^+(1260)$ in reasonable agreement with experiment. But once again we caution about determining fit fractions of these resonances given the large interferences found.

The other finding of our study is that thanks to the explicit consideration of resonances as coming from meson-meson scattering in coupled channels, we could reproduce the data starting with mechanisms of external and internal emission and do not need to invoke a weak annihilation mechanism. This is because even if some resonances are not produced in a first step through external or internal emission, some of the coupled channels, different to the state observed at the end, can be produced. The rescattering produces the desired final state, while at the same time generates some resonances.

We also perform a study of the uncertainties of our fit concluding that the fit parameters have large uncertainties but there are strong correlations between them such that the uncertainties in the fit are small. This also indicates that the small discrepancies found with the data should find an explanation beyond the theoretical framework that we have done.

ACKNOWLEDGMENTS

J. S. would like to thank Dr. Jun-Xu Lu for useful discussions. This work is partly supported by the Spanish Ministerio de Economia y Competitividad (MINECO) and European FEDER funds under Contract No. PID2020–112777 GB-I00, and by Generalitat Valenciana under Contract No. PROMETEO/2020/023. This project has received funding from the European Union Horizon 2020 research and innovation programme under the program H2020-INFRAIA-2018-1, Grant Agreement No. 824093 of the STRONG-2020 project. J. S. wishes to acknowledge support from China Scholarship Council. The work of A. F. was partially supported by the Generalitat Valenciana and European Social Fund APOSTD-2021-112, and the Czech Science Foundation, GAČR Grant No. 19-19640S.

[1]Technically we should remove 16% of the values obtained for each distribution in both extremes to get 68% confidence level, but this only makes the band a bit narrower.

[1] D. R. Boito and R. Escribano, Phys. Rev. D **80**, 054007 (2009).
[2] P. C. Magalhaes, M. R. Robilotta, K. S. F. F. Guimaraes, T. Frederico, W. de Paula, I. Bediaga, A. C. d. Reis, C. M. Maekawa, and G. R. S. Zarnauskas, Phys. Rev. D **84**, 094001 (2011).
[3] J. P. Dedonder, R. Kaminski, L. Lesniak, and B. Loiseau, Phys. Rev. D **89**, 094018 (2014).
[4] J.-J. Xie, L.-R. Dai, and E. Oset, Phys. Lett. B **742**, 363 (2015).
[5] P. C. Magalhães and M. R. Robilotta, Phys. Rev. D **92**, 094005 (2015).
[6] T. Sekihara and E. Oset, Phys. Rev. D **92**, 054038 (2015).
[7] J. M. Dias, F. S. Navarra, M. Nielsen, and E. Oset, Phys. Rev. D **94**, 096002 (2016).
[8] S. Sakai, E. Oset, and W. H. Liang, Phys. Rev. D **96**, 074025 (2017).
[9] F. Niecknig and B. Kubis, Phys. Lett. B **780**, 471 (2018).
[10] R. Molina, J.-J. Xie, W.-H. Liang, L.-S. Geng, and E. Oset, Phys. Lett. B **803**, 135279 (2020).
[11] Y.-K. Hsiao, Y. Yu, and B.-C. Ke, Eur. Phys. J. C **80**, 895 (2020).
[12] M.-Y. Duan, J.-Y. Wang, G.-Y. Wang, E. Wang, and D.-M. Li, Eur. Phys. J. C **80**, 1041 (2020).
[13] L. Roca and E. Oset, Phys. Rev. D **103**, 034020 (2021).
[14] G. Toledo, N. Ikeno, and E. Oset, Eur. Phys. J. C **81**, 268 (2021).
[15] E. Oset *et al.*, Int. J. Mod. Phys. E **25**, 1630001 (2016).
[16] M. Ablikim *et al.* (BESIII Collaboration), Phys. Rev. D **104**, 071101 (2021).
[17] L.-L. Chau, Phys. Rep. **95**, 1 (1983).
[18] L.-L. Chau and H.-Y. Cheng, Phys. Rev. D **36**, 137 (1987); **39**, 2788(A) (1989).
[19] M. Ablikim *et al.* (BESIII Collaboration), Phys. Rev. Lett. **123**, 112001 (2019).
[20] X.-Z. Ling, M.-Z. Liu, J.-X. Lu, L.-S. Geng, and J.-J. Xie, Phys. Rev. D **103**, 116016 (2021).
[21] Y. Yu, Y.-K. Hsiao, and B.-C. Ke, Eur. Phys. J. C **81**, 1093 (2021).
[22] J. A. Oller and E. Oset, Nucl. Phys. **A620**, 438 (1997); **A652**, 407(E) (1999).
[23] N. Kaiser, Eur. Phys. J. A **3**, 307 (1998).
[24] M. P. Locher, V. E. Markushin, and H. Q. Zheng, Eur. Phys. J. C **4**, 317 (1998).
[25] J. Nieves and E. Ruiz Arriola, Nucl. Phys. **A679**, 57 (2000).
[26] M. F. M. Lutz and E. E. Kolomeitsev, Nucl. Phys. **A730**, 392 (2004).
[27] L. Roca, E. Oset, and J. Singh, Phys. Rev. D **72**, 014002 (2005).
[28] L. S. Geng, E. Oset, L. Roca, and J. A. Oller, Phys. Rev. D **75**, 014017 (2007).
[29] Y. Zhou, X.-L. Ren, H.-X. Chen, and L.-S. Geng, Phys. Rev. D **90**, 014020 (2014).
[30] A. Bramon, A. Grau, and G. Pancheri, Phys. Lett. B **283**, 416 (1992).
[31] W. H. Liang and E. Oset, Phys. Lett. B **737**, 70 (2014).
[32] P. A. Zyla *et al.* (Particle Data Group), Prog. Theor. Exp. Phys. **2020**, 083C01 (2020).
[33] P. Rubin *et al.* (CLEO Collaboration), Phys. Rev. Lett. **93**, 111801 (2004).
[34] M. Ablikim *et al.* (BESIII Collaboration), Phys. Rev. D **95**, 032002 (2017).
[35] J.-J. Wu, Q. Zhao, and B. S. Zou, Phys. Rev. D **75**, 114012 (2007).
[36] C. Hanhart, B. Kubis, and J. R. Pelaez, Phys. Rev. D **76**, 074028 (2007).
[37] L. Roca, Phys. Rev. D **88**, 014045 (2013).
[38] F. Aceti, W. H. Liang, E. Oset, J. J. Wu, and B. S. Zou, Phys. Rev. D **86**, 114007 (2012).
[39] S. Weinberg, Phys. Rev. **137**, B672 (1965).
[40] V. Baru, C. Hanhart, Y. S. Kalashnikova, A. E. Kudryavtsev, and A. V. Nefediev, Eur. Phys. J. A **44**, 93 (2010).
[41] T. Kinugawa and T. Hyodo, EPJ Web Conf. **262**, 01019 (2022).
[42] Y. Li, F.-K. Guo, J.-Y. Pang, and J.-J. Wu, Phys. Rev. D **105**, L071502 (2022).
[43] J. Song, L. R. Dai, and E. Oset, Eur. Phys. J. A **58**, 133 (2022).
[44] M. Albaladejo and J. Nieves, Eur. Phys. J. C **82**, 724 (2022).
[45] P. C. Bruns, arXiv:2203.16909.
[46] H. Toki, C. Garcia-Recio, and J. Nieves, Phys. Rev. D **77**, 034001 (2008).
[47] D. Gamermann, J. Nieves, E. Oset, and E. Ruiz Arriola, Phys. Rev. D **81**, 014029 (2010).
[48] Z.-F. Sun, M. Bayar, P. Fernandez-Soler, and E. Oset, Phys. Rev. D **93**, 054028 (2016).
[49] L. D. Landau, Nucl. Phys. **13**, 181 (1959).
[50] M. Bayar, F. Aceti, F.-K. Guo, and E. Oset, Phys. Rev. D **94**, 074039 (2016).
[51] J. A. Oller and E. Oset, Phys. Rev. D **60**, 074023 (1999).
[52] A. Martinez Torres, K. P. Khemchandani, L. Roca, and E. Oset, Few Body Syst. **61**, 35 (2020).
[53] A. Martinez Torres, K. P. Khemchandani, D. Jido, and A. Hosaka, Phys. Rev. D **84**, 074027 (2011).
[54] B. Efron and R. Tibshirani, Stat. Sci. **57**, 54 (1986).
[55] M. Albaladejo *et al.* (JPAC Collaboration), Prog. Part. Nucl. Phys. 103981 (2021).
[56] J. Landay, M. Döring, C. Fernández-Ramírez, B. Hu, and R. Molina, Phys. Rev. C **95**, 015203 (2017).
[57] R. Navarro Pérez, J. E. Amaro, and E. Ruiz Arriola, Phys. Lett. B **738**, 155 (2014).
[58] J.-J. Xie, W.-H. Liang, and E. Oset, Eur. Phys. J. A **55**, 6 (2019).
[59] J. Brownlee, A gentle introduction to statistical sampling and resampling (2018), https://machinelearningmastery.com/statistical-sampling-and-resampling/.
[60] B. LeBeau and Z. A. S., Statistical reasoning through computation and R (2022), https://lebebr01.github.io/stat_thinking/.